R-926 4

April 1989

By L.J. Malvar (UCLA) and
G.E. Warren (NCEL)

Sponsored By Chief of
Naval Research

NCEL
Technical Report

ANALYTICAL MODELING OF REINFORCED CONCRETE IN TENSION

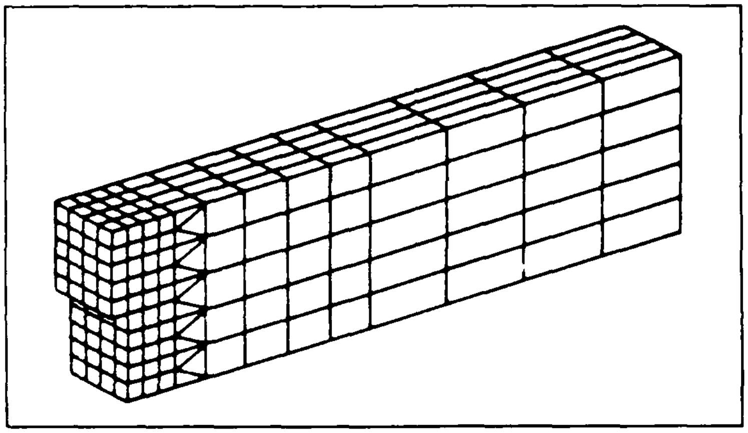

ABSTRACT A smeared crack approach to fracture of concrete in mode I was implemented in the finite element program ADINA. Nonlinear concrete elements with tensile cracking were modified to include tensile strain softening. When an element at an integration point cracks, the stiffness perpendicular to the crack is reduced to zero and the tensile stress across it is set as a function of the crack opening. Equilibrium iterations were implemented to redistribute stress. Two- and three-dimensional models of a single edge notched beam in three-point bending were analyzed and compared to experimental results with good agreement. The analytical representation of mixed mode fracture was also addressed. The mechanisms of shear transfer across a crack were detailed, and the rough crack model, relating shear stress to crack opening, is presented with discussions on orientation of successive crack planes, tensorial invariance, and snap-back phenomena. Problems are identified with modeling bond at the concrete/reinforcement interface and its effect on crack patterns.

NAVAL CIVIL ENGINEERING LABORATORY PORT HUENEME CALIFORNIA 93043

89 6 07 010

METRIC CONVERSION FACTORS

Approximate Conversions to Metric Measures

Symbol	When You Know	Multiply by	To Find	Symbol
		LENGTH		
in	inches	*2.5	centimeters	cm
ft	feet	30	centimeters	cm
yd	yards	0.9	meters	m
mi	miles	1.6	kilometers	km
		AREA		
in^2	square inches	6.5	square centimeters	cm^2
ft^2	square feet	0.09	square meters	m^2
yd^2	square yards	0.8	square meters	m^2
mi^2	square miles	2.6	square kilometers	km^2
	acres	0.4	hectares	ha
		MASS (weight)		
oz	ounces	28	grams	g
lb	pounds	0.45	kilograms	kg
	short tons (2,000 lb)	0.9	tonnes	t
		VOLUME		
tsp	teaspoons	5	milliliters	ml
Tbsp	tablespoons	15	milliliters	ml
fl oz	fluid ounces	30	milliliters	ml
c	cups	0.24	liters	l
pt	pints	0.47	liters	l
qt	quarts	0.95	liters	l
gal	gallons	3.8	liters	l
ft^3	cubic feet	0.03	cubic meters	m^3
yd^3	cubic yards	0.76	cubic meters	m^3
		TEMPERATURE (exact)		
°F	Fahrenheit temperature	5/9 (after subtracting 32)	Celsius temperature	°C

*1 in = 2.54 (exactly). For other exact conversions and more detailed tables, see NBS Misc. Publ. 286, Units of Weights and Measures, Price $2.25, SD Catalog No. C13.10:286.

Approximate Conversions from Metric Measures

Symbol	When You Know	Multiply by	To Find	Symbol
		LENGTH		
mm	millimeters	0.04	inches	in
cm	centimeters	0.4	inches	in
m	meters	3.3	feet	ft
m	meters	1.1	yards	yd
km	kilometers	0.6	miles	mi
		AREA		
cm^2	square centimeters	0.16	square inches	in^2
m^2	square meters	1.2	square yards	yd^2
km^2	square kilometers	0.4	square miles	mi^2
ha	hectares (10,000 m^2)	2.5	acres	
		MASS (weight)		
g	grams	0.035	ounces	oz
kg	kilograms	2.2	pounds	lb
t	tonnes (1,000 kg)	1.1	short tons	
		VOLUME		
ml	milliliters	0.03	fluid ounces	fl oz
l	liters	2.1	pints	pt
l	liters	1.06	quarts	qt
l	liters	0.26	gallons	gal
m^3	cubic meters	35	cubic feet	ft^3
m^3	cubic meters	1.3	cubic yards	yd^3
		TEMPERATURE (exact)		
°C	Celsius temperature	9/5 (then add 32)	Fahrenheit temperature	°F

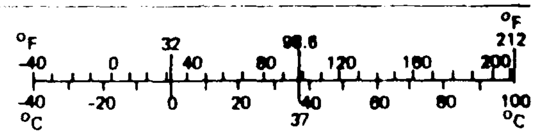

Unclassified

SECURITY CLASSIFICATION OF THIS PAGE (When Data Entered)

REPORT DOCUMENTATION PAGE		READ INSTRUCTIONS BEFORE COMPLETING FORM
1. REPORT NUMBER TR-926	2. GOVT ACCESSION NO DN665019	3. RECIPIENT'S CATALOG NUMBER
4. TITLE (and Subtitle) ANALYTICAL MODELING OF REINFORCED CONCRETE IN TENSION		5. TYPE OF REPORT & PERIOD COVERED Not Final; Oct 1987 - Sep 1988 6. PERFORMING ORG. REPORT NUMBER
7. AUTHOR(s) L.J. Malvar, UCLA and G.E. Warren, NCEL		8. CONTRACT OR GRANT NUMBER(s)
9. PERFORMING ORGANIZATION NAME AND ADDRESS NAVAL CIVIL ENGINEERING LABORATORY Port Hueneme, California 93043-5003		10. PROGRAM ELEMENT, PROJECT, TASK AREA & WORK UNIT NUMBERS 61153N; YR023.03.01B
11. CONTROLLING OFFICE NAME AND ADDRESS Chief of Naval Research Arlington, Virginia 22217-5000		12. REPORT DATE April 1989 13. NUMBER OF PAGES 48
14. MONITORING AGENCY NAME & ADDRESS (if different from Controlling Office)		15. SECURITY CLASS (of this report) Unclassified 15a. DECLASSIFICATION DOWNGRADING SCHEDULE

16. DISTRIBUTION STATEMENT (of this Report)

Approved for public release; distribution is unlimited.

17. DISTRIBUTION STATEMENT (of the abstract entered in Block 20, if different from Report)

18. SUPPLEMENTARY NOTES

19. KEY WORDS (Continue on reverse side if necessary and identify by block number)

Concrete, fracture mechanisms, crack propagation, mixed mode, shear, bond tension, ~~finite elements~~, softening, fracture energy, ADINA

20. ABSTRACT (Continue on reverse side if necessary and identify by block number)

A smeared crack approach to fracture of concrete in mode I was implemented in the finite element program ADINA. Nonlinear concrete elements with tensile cracking were modified to include tensile strain softening. When an element at an integration point cracks, the stiffness perpendicular to the crack is reduced to zero and the tensile stress across it is set as a function of the crack opening. Equilibrium iterations were implemented to redistribute stress. Two- and three-dimensional models of a single edge notched beam in

Continued

20. Continued

three-point bending were analyzed and compared to experimental results with good agreement. The analytical representation of mixed mode fracture was also addressed. The mechanisms of shear transfer across a crack were detailed, and the rough crack model, relating shear stress to crack opening, is presented with discussions on orientation of successive crack planes, tensorial invariance, and snap-back phenomena. Problems are identified with modeling bond at the concrete/reinforcement interface and its effect on crack patterns.

Library Card

Naval Civil Engineering Laboratory
ANALYTICAL MODELING OF REINFORCED CONCRETE IN TENSION (Not Final), by L.J. Malvar and G.E. Warren
TR-926 48 pp illus Apr 1989 Unclassified

1. Concrete 2. Fracture mechanisms I. YR023.03.01B

A smeared crack approach to fracture of concrete in mode I was implemented in the finite element program ADINA. Nonlinear concrete elements with tensile cracking were modified to include tensile strain softening. When an element at an integration point cracks, the stiffness perpendicular to the crack is reduced to zero and the tensile stress across it is set as a function of the crack opening. Equilibrium iterations were implemented to redistribute stress. Two and three-dimensional models of a single edge notched beam in three-point bending were analyzed and compared to experimental results with good agreement. The analytical representation of mixed mode fracture was also addressed. The mechanisms of shear transfer across a crack were detailed, and the rough crack model, relating shear stress to crack opening, is presented with discussions on orientation of successive crack planes, tensorial invariance, and snap-back phenomena. Problems are identified with modeling bond at the concrete/reinforcement interface and its effect on crack patterns.

CONTENTS

PURPOSE

The Office of Naval Research (ONR) through the Naval Civil Engineering Laboratory (NCEL) has initiated a project to develop fracture mechanics methodology for design application of reinforced concrete elements in tensile and shear stress states. Since completion of an experimental program to establish the fracture energy parameters of plain concrete reported in Reference 1, efforts have been directed to the analytical formulation and modeling of tensile behavior of concrete. The purpose of this report is to present analytical modeling methodology of mode I (crack opening), mixed mode crack propagation (shear), and concrete reinforcing interface behavior (bond).

This report supports the project "Fatigue and Fracture of Concrete" in the ONR 6.1 Basic Research Program YR023.03.01B, Structural Modeling. In addition to design and analysis applications, concrete fracture mechanics methodology will eventually be incorporated into damage and condition assessment process of existing in service reinforced concrete facilities.

Concrete cracking in tension is the major factor contributing to the nonlinear behavior of reinforced concrete elements. The modeling of cracking in shear-critical members is most important since it will determine the ultimate resistance and post-failure behavior.

Crack propagation is facilitated when the material is in a state of plane strain. The material of thick members is in a state close to plane strain in the interior and in a state of plane stress along the edges. An accurate representation of the cracking will be obtained only if three-dimensional effects are considered. In the first part of this report a smeared crack representation is formulated and implemented in the two- and three-dimensional nonlinear concrete elements of the computer code ADINA (Ref 2). Experimental results from tests carried out on single edge notched beams show good agreement when compared to the analytical predictions.

Fracture of concrete may occur in three ways: Mode I (opening), II (shearing) and III (tearing). Although pure modes may be encountered, mixed mode propagation is more likely. In the second part of this report existing models of mode II and mixed mode constitutive relations are evaluated. Mixed mode crack propagation involves considering the transfer of shear forces across cracks. As a consequence, successive crack planes may form; these need not be orthogonal to each other. This report also addresses the analysis of shear transfer across cracks.

Crack distribution is greatly affected by the reinforcement-concrete interface behavior. Proper modeling of the bond stress-slip relationship is needed for an accurate prediction of the crack pattern. Bond-slip is addressed in the third part of the report.

The modifications implemented in ADINA in each case have been compiled in Appendixes A, B, and C.

PART 1. THREE-DIMENSIONAL MODE I CRACK PROPAGATION

INTRODUCTION

Finite element modeling of concrete fracture mechanics is a versatile tool for analysis. The implementation of a nonlinear discrete crack model has already been evaluated (Ref 1). However, discrete crack models present the difficulty of varying mesh topology to represent the crack advance. Modeling the crack advance is further complicated if the analysis is three-dimensional.

A smeared crack or crack band approach was implemented in the finite element program ADINA (Ref 2). The fracture zone was modeled as a band of uniformly distributed parallel microcracks having a blunt front. This concept was pioneered by Rashid (Ref 3), developed by Bazant et al. (Ref 4 through 7), and is also known as the Crack Band Model (CBM).

After implementation of the CBM approach into the two- and three-dimensional (2-D and 3-D) nonlinear concrete elements of ADINA, the performance of the models was evaluated by analyzing the results of the test series reported in Reference 1.

THE SMEARED CRACK APPROACH

Numerous experiments conducted on tensile specimens have shown that after crack formation, tensile stresses are transferred across the crack and their magnitude decreases with crack opening. Two stress-versus-crack width relationships have been formulated that are suitable for finite element applications. The Fictitious Crack Model (FCM) (Ref 8) represents a single crack development by separating the elements via introduction of new nodes and imposes nodal forces equivalent to the transferred stresses. The Crack Band Model transforms the crack opening, w, into strain, ε, dividing it by the element width and obtaining an equivalent stress versus strain ($\sigma - \varepsilon$) relationship.

The CBM approach assumes that cracked elements show a strain softening behavior; i.e., the element stiffness is negative. This leads to a stiffness matrix not definitely positive, which would make the solution of finite element equations difficult and result in large errors. Strain softening in ADINA is included for concrete elements subjected to stresses beyond the maximum compressive stress. Upon reaching maximum compressive stress, zero (very small) stiffness is assigned coupled with isotropic conditions, and the stress increments are computed from a uniaxial stress-versus strain law. A similar approach can be implemented in tension. Upon cracking at an integration point, a zero stiffness can be assigned across the crack and the stress increments can be derived from an equivalent, empirical stress-versus-strain law. The tensile model becomes orthotropic (Ref 9). Iterations are then required to satisfy equilibrium.

While transforming the stress-versus-crack-width relationship (σ - w) to stress-versus-strain (σ - ε), the element width is included, resulting in a solution dependent on element size. In order to circumvent this condition, Bazant and Cedolin (Ref 5) suggested linking the relationship to the fracture energy, G_f, forcing the empirical σ - ε law to verify

$$G_f = h \int_0^{\varepsilon_o} \sigma \, d\varepsilon \tag{1}$$

where h is the band width, ε the strain and ε_o the strain beyond which no stress is transferred. It is implied that the fracture energy (the energy needed to create a unit fracture area along the crack path) is uniformly distributed across the width of the fracture zone (band width).

Equation (1) is verified if

$$\sigma/f_t = f(w/w_o) \tag{2}$$

which satisfies

$$G_f = \int_0^{w_o} \sigma \, dw = w_o f_t \int_0^1 \sigma/f_t \, d(w/w_o) \tag{3}$$

where

w = crack width or crack opening

w_o = crack width beyond which no stress is transferred

f_t = tensile strength

and

$$w/w_c = \varepsilon - \sigma/E$$

$$w_o/w_c = \varepsilon_o$$

$$w/w_o = (\varepsilon - \sigma/E)/\varepsilon_o = \varepsilon/\varepsilon_o - (\sigma/f_t)(f_t/\varepsilon_o E)$$

$$= \varepsilon/\varepsilon_o - (\sigma/f_t)(\varepsilon_p/\varepsilon_o) \tag{4}$$

where

w_c = element width

E = Young's modulus of concrete

ε_p = the strain corresponding to tensile strength

Substituting Equation (4) into Equation (2) yields:

$$\sigma/f_t = f(\varepsilon/\varepsilon_o, \sigma/f_t)$$

In general it is difficult to explicitly obtain stress.

In Reference 1, different $\sigma - w$ laws were evaluated. A more recent one has been presented by Cornelissen et al. (Ref 10) and used by others (Ref 11 and 12). This nonlinear relationship and one describing linear softening are described in following sections and have been implemented in ADINA.

STRESS - STRAIN LAWS

Linear Softening

In spite of numerous tests on tensile specimens (Ref 10, 13, and 14) showing a highly nonlinear softening, linear softening is sometimes used for computational simplicity. Typically the stress declines sharply upon crack initiation, up to an opening of approximately 15 x 10^{-3} mm beyond which the decline is not pronounced. The importance of the type of relationship used was pointed out in Reference 1 and will also be demonstrated in the present study.

A constant negative softening modulus, E_t, can be defined for linear softening and $\varepsilon > \varepsilon_p$ as

$$E_t = \frac{1}{\frac{1}{E} - \frac{2G_f}{w_c f_t^2}} \qquad (5)$$

E_t and the $\sigma - \varepsilon$ law are shown in Figure 1a.

Nonlinear Softening

The nonlinear $\sigma - w$ relationship defined in Reference 10 is shown in a nondimensional form in Figure 1b. It is an empirical formula derived by curve fitting the results of tensile tests.

$$\sigma/f_t = \{1+(C_1 w/w_o)^3\}e^{(-C_2 w/w_o)} - w/w_o(1+C_1^{\,3})e^{(-C_2)} \qquad (6)$$

where $C_1 = 3$ and $C_2 = 6.93$.

From Equation (3) w_o can be found since G_f and f_t are known from experimental results as described in the following sections. From Equation (6):

$$\int_0^1 \sigma/f_t \, d(w/w_o) = 0.19470$$

To obtain a stress-versus-strain law, several points $(w/w_o, \sigma/f_t)$ were chosen from Equation (6) (see Table 1) and transformed into $(\varepsilon/\varepsilon_o, \sigma/f_t)$. Linear interpolation was then performed between data points.

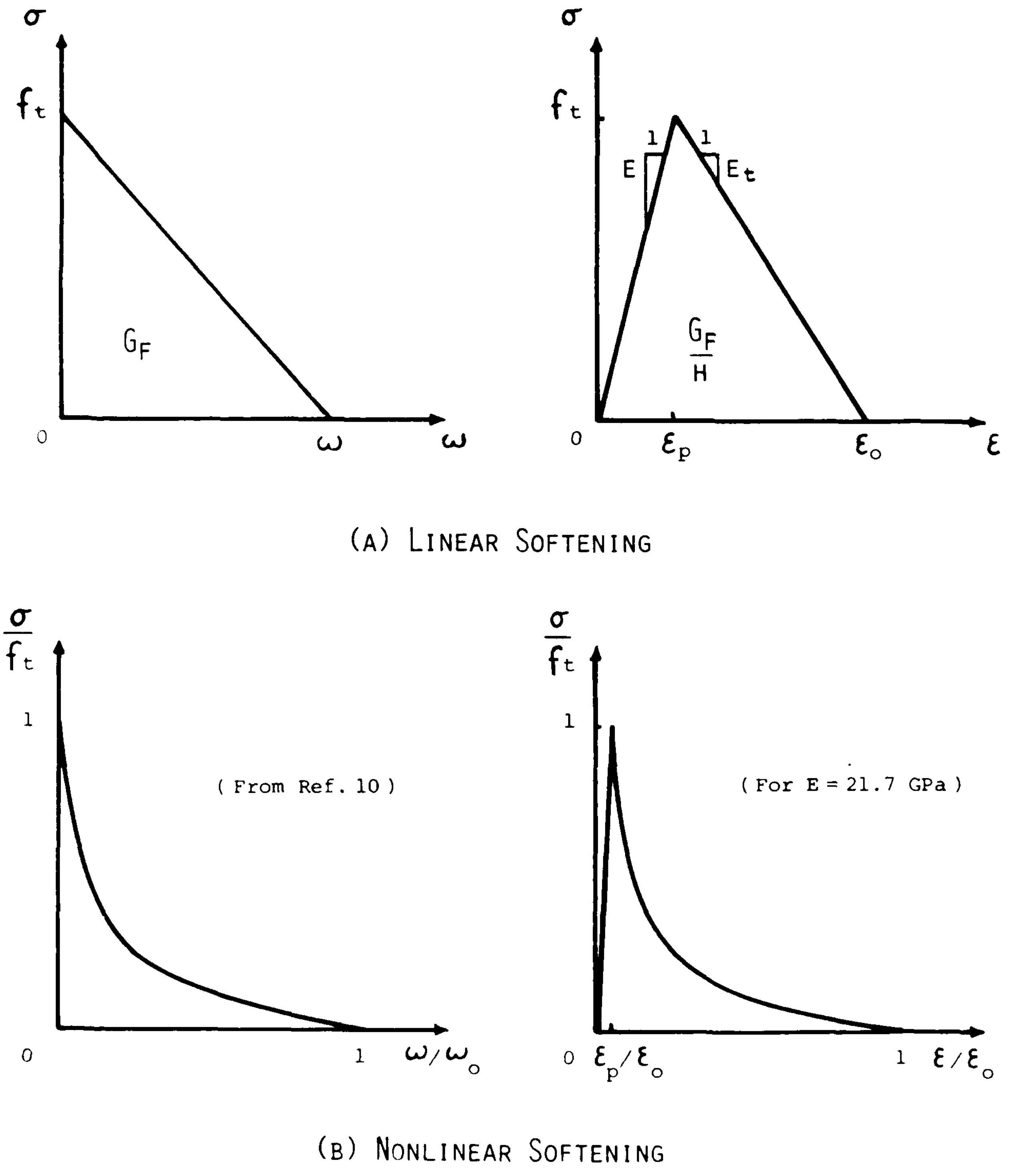

Figure 1. Stress versus crack width and stress versus strain relationships.

Table 1. Stress - Crack Width Relationship (from Ref 10)

w/w_o	σ/f_t
0.00	1.0000
0.05	0.7082
0.10	0.5108
0.15	0.3817
0.20	0.2986
0.25	0.2446
0.30	0.2080
0.40	0.1596
0.60	0.0904
0.80	0.0361
1.00	0.0000

For the linear approximation:

$$\int_0^1 \sigma/f_t \, d(w/w_o) = 0.19704$$

Since $w_o = w_c \varepsilon_o$ and $h = 2w_c$ (two elements were chosen across the crack band), ε_o is found from

$$G_f/2 = 0.19704 \, w_c \, \varepsilon_o \, f_t$$

TEST SERIES

Twelve single edge notched beams with dimensions 102 mm by 102 mm (4 in. by 4 in.) cross section, 838 mm (33 in.) length and 788 mm (31 in.) span were tested in three point bending. The notch-to-depth ratio, a_o/W, was 0.5. The maximum aggregate size, d_a, was 9.5 mm (3/8 in.). The tests were carried out in displacement control.

Concrete properties are indicated in Table 2. The compressive strength was measured at 28 days on three 105 mm diameter by 305 mm (6 in. by 12 in.) standard cylinders. The tensile strength was obtained from splitting tensile tests conducted at 28 days on six similar cylinders. At the initiation of the compression tests strain readings at the cylinders' mid-height yielded the modulus of elasticity.

The results which have been reported in detail earlier (Ref 1) are summarized in Table 3. The fracture energy was obtained as the area under the load versus load-point deflection plot divided by the cross

Table 2. Concrete Properties

Ingredient	Amount
cement	279 kg/m^3
water	167 kg/m^3
9.5 mm gravel	1062 kg/m^3
sand	907 kg/m^3

Compressive strength at 28 days, f'_c = 29.0 MPa

Tensile strength at 28 days, f_t = 3.1 MPa

Modulus of elasticity, E = 21.7 GPa

sectional area at the notch. Also indicated are the mid-span displacements at peak load, d_p, and at the end of the test, d_o (when the load carrying capacity of the beam vanishes). The set-up used is shown in Figure 2. An average of all experimental LLPD plots was used to compare with results from material modeling using the finite element method.

FINITE ELEMENT ANALYSIS

The average value of the fracture energy, G_f, was 0.0763 N/mm. Values obtained showed some variation with size and configuration.

Isoparametric elements and Gaussian integration were used. The smallest number possible of integration points was used (2 x 2 for two dimensions, 2 x 2 x 2 for three dimensions) to compensate for the excessive stiffness of these elements (Ref 15).

During crack propagation, the stiffness matrix had to be reformed periodically to reflect the changes of stiffness in the cracked elements (Ref 15 and 16). Stiffness was reformed at every equilibrium iteration for each loading step (a full Newton-Raphson procedure was employed). This approach inherently leads to a step-size dependency; that is if the loading steps are too large then too few reformations will be performed (Ref 17). Results appeared to remain practically constant for displacement steps below 0.0125 mm.

Although shear transfer across a crack can be modeled in ADINA through the use of a shear retention factor, ß, no shear should be present in the center section of the symmetric specimen. To avoid energy consumption a very low value of ß (0.0001) was adopted. It should be noted that recent research is drifting away from a constant shear retention factor towards a shear softening approach (Ref 12).

Table 3. Experimental Results

Specimen	G_f (N/m)	Peak load (N)	d_p (mm)	d_o (mm)
1	72.3	853	0.17	2.8
2	79.7	999	0.18	2.4
3	85.6	945	0.19	2.8
4	70.5	820	0.17	2.2
5	75.7	910	0.15	3.1
6	72.4	921	0.15	2.2
7	83.4	1011	0.16	2.5
8	75.3	950	0.17	2.9
9	68.1	883	0.13	2.4
10	68.6	950	0.16	2.6
11	84.1	950	0.16	2.7
12	79.8	997	0.15	2.0
Mean	76.3	932	0.16	2.6
Standard Deviation	6.1			

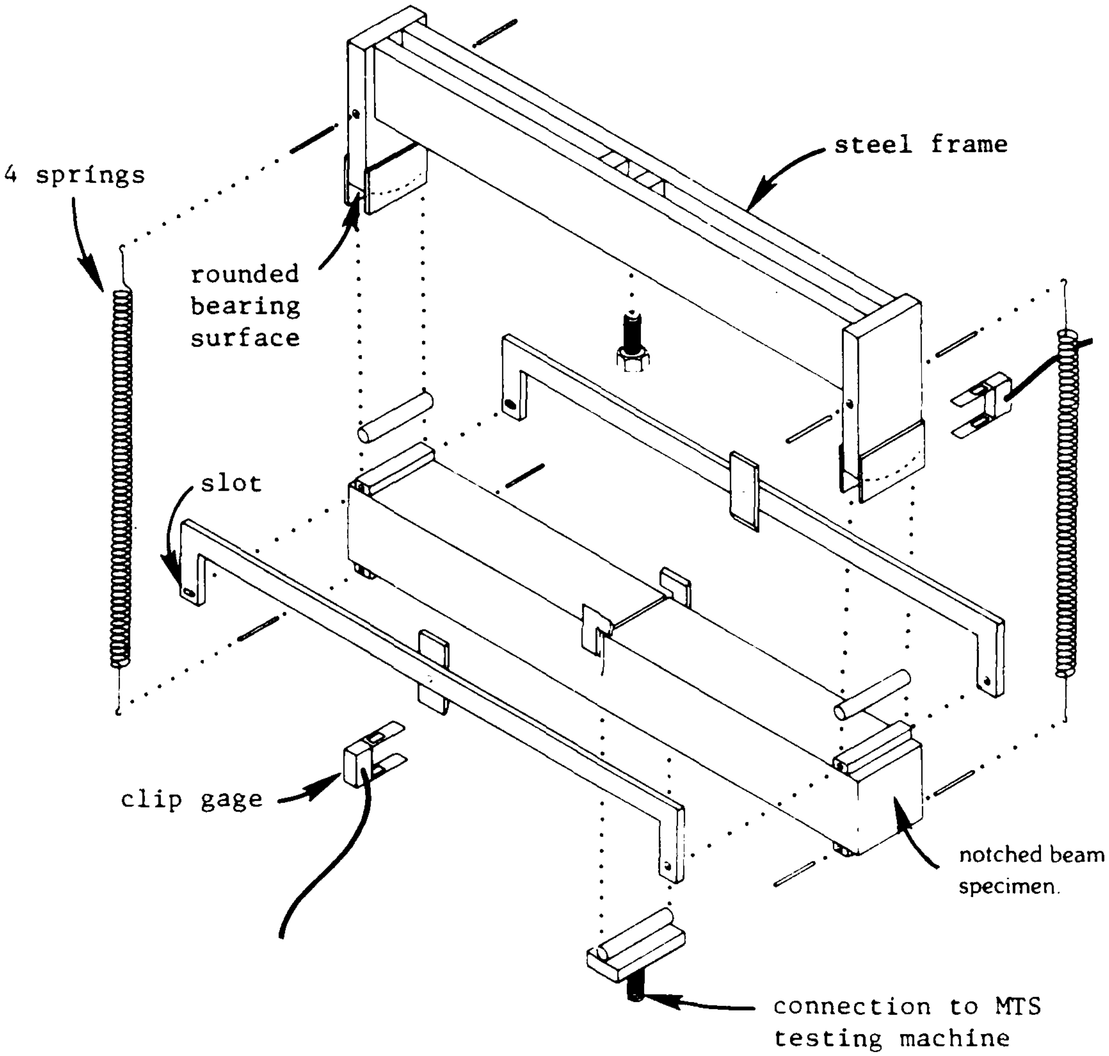

Figure 2. Test set-up.

Optimum configuration for a finite element is a square (2-D) or a cube (3-D). The element dimensions in the fracture zone were then chosen as 10 mm by 10 mm (2-D) or 10 mm by 10 mm by 10 mm (3-D). The crack band width was then 20 mm which is 2.1 times the maximum aggregate size d_a and is consistent with Reference 6, which found an optimum value of the crack band width to be around $3d_a$. Finite element meshes are shown in Figure 3.

The 2-D mesh used for the crack bond model is shown in Figure 3a. Only half of the specimen is discretized due to symmetry. In the C model, only nonlinear elements are used. In the LE model, only the five elements ahead of the notch are nonlinear concrete elements, all the others are linear elastic (LE model).

The 3-D mesh used is shown in Figure 3c. Only one quarter of the specimen is discretized due to the double symmetry. Two cases were again considered: LE, with 20 concrete and 500 elastic elements, and C, with all concrete elements.

FINITE ELEMENT RESULTS

Two-Dimensional Model

To compare with experimental observations (curve EXP of Figure 4), the LE model was first analyzed using a linear softening (LE-LS) and Cornelissen's relationship (LE-CS). Both load-load point deflation (LLPD) responses are shown on Figure 4. In addition, results using linear elastic elements, linear softening and the Fictitious Crack Model from Reference 1 are also shown (FCM-LE-LS). The mesh used with the FCM is shown in Figure 3b. Appendixes A and B detail the implementation of the FCM and the two-dimensional CBM.

The C model was then analyzed using Cornelissen's softening, and results are shown with the corresponding response from the others (C-CS). The magnified deformed shape is shown in Figure 5.

Three-Dimensional Model

LLPD plots for both LE and C three-dimensional models are shown in Figure 6 along with experimental response. Only nonlinear softening was used and the corresponding responses are marked LE-CS and C-CS. Numerical and graphic results shown in Figure 7 were obtained at peak load with the C-CS model. The magnified deformed shape of the cross section at the notch is shown in Figure 7a (due to symmetry only half of it is actually shown), while Figure 7b presents the stresses transferred across the cracked elements (at the integration points). Appendix C details the implementation of the three-dimensional CBM.

DISCUSSION

Two-Dimensional Model

Initial stiffness. It appears from Figure 4 that the CBM approach yields an initial stiffness which is about 10% lower than the experimental value. First cracking occurs at a load of about 600 N. Since

most of the elements are linear elastic, the initial response of the model is governed primarily by mesh geometry and element size. While the FCM analysis used a fine mesh (205 elements) with a zero notch width (Figure 3b), the CBM mesh is much coarser (90 elements) and shows a notch 20 mm wide (Figure 3a). A better match might be possible if the mesh was refined; however, the element should not be made smaller than the aggregate size. Another possible improvement would be to choose only one element across the whole crack band, cutting the notch size to 10 mm. However the latter would result in loss of model symmetry and the entire beam would have to be discretized.

Linear elastic elements with linear softening. Figure 4 indicates that the FCM and CBM yield essentially equivalent results (curves LE-LS and FCM-LE-LS). Both theories assume the total energy needed to fracture the specimen to be distributed uniformly along the fracture surface. A better match between them would be obtained if the meshes were equally refined. The simplification introduced by considering linear strain softening yields responses further from the experimental data than obtained with nonlinear softening.

Nonlinear softening. Using linear elastic elements with Cornelissen's nonlinear stress versus displacement relationship yields a response closer to the experimental behavior (curve LE- CS). Further refinement with exclusive application of nonlinear concrete elements results in only a slight response change from the linear elastic case (curve C-CS).

Three-Dimensional Model

Three-dimensional isoparametric elements are stiffer than two-dimensional ones. As a consequence the initial behavior is closer to the experimental data as shown in Figure 6. After cracking, the load obtained for each displacement step is slightly lower than in the 2-D case.

The use of only nonlinear concrete elements (C-CS) increased the computing time threefold but did not affect substantially the response. The predicted peak load was in both cases lower than the experimental value (16% for C-CS versus 13% for LE-CS). It is reasonable to expect similarity since the nonlinear behavior concentrates near the fracture plane and the crack tip.

Figure 7b shows the stresses transferred across the cracked elements. It is apparent that more stress is transferred towards the beam's free edges. It is concluded that the crack at the edges does not open as wide and propagates slower than at the center (which typically occurs with metals). However, this deviation is small and the crack front can be assumed to be straight.

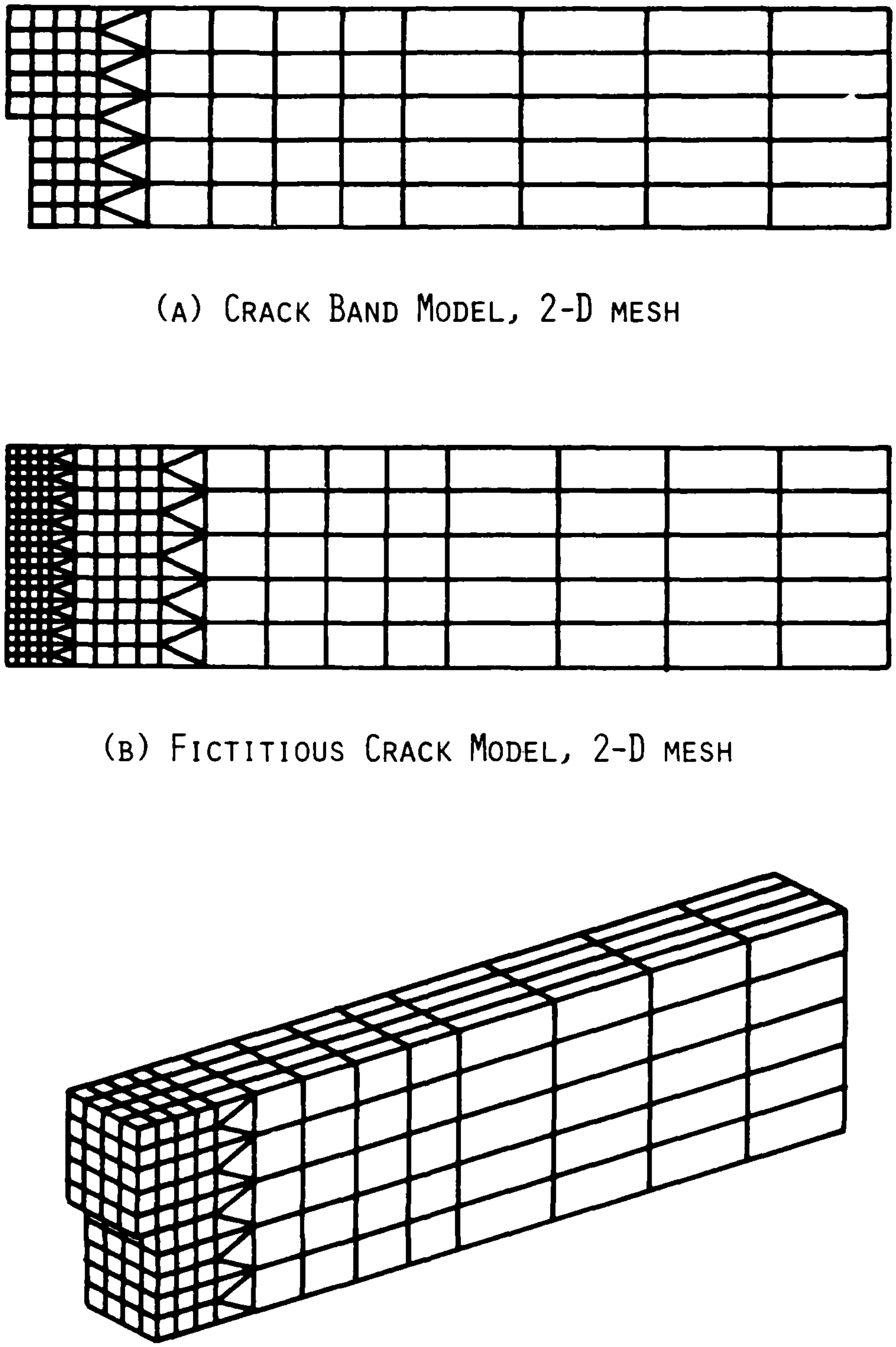

(a) Crack Band Model, 2-D mesh

(b) Fictitious Crack Model, 2-D mesh

(c) Crack Band Model, 3-D mesh

Figure 3. Two- and three-dimensional models.

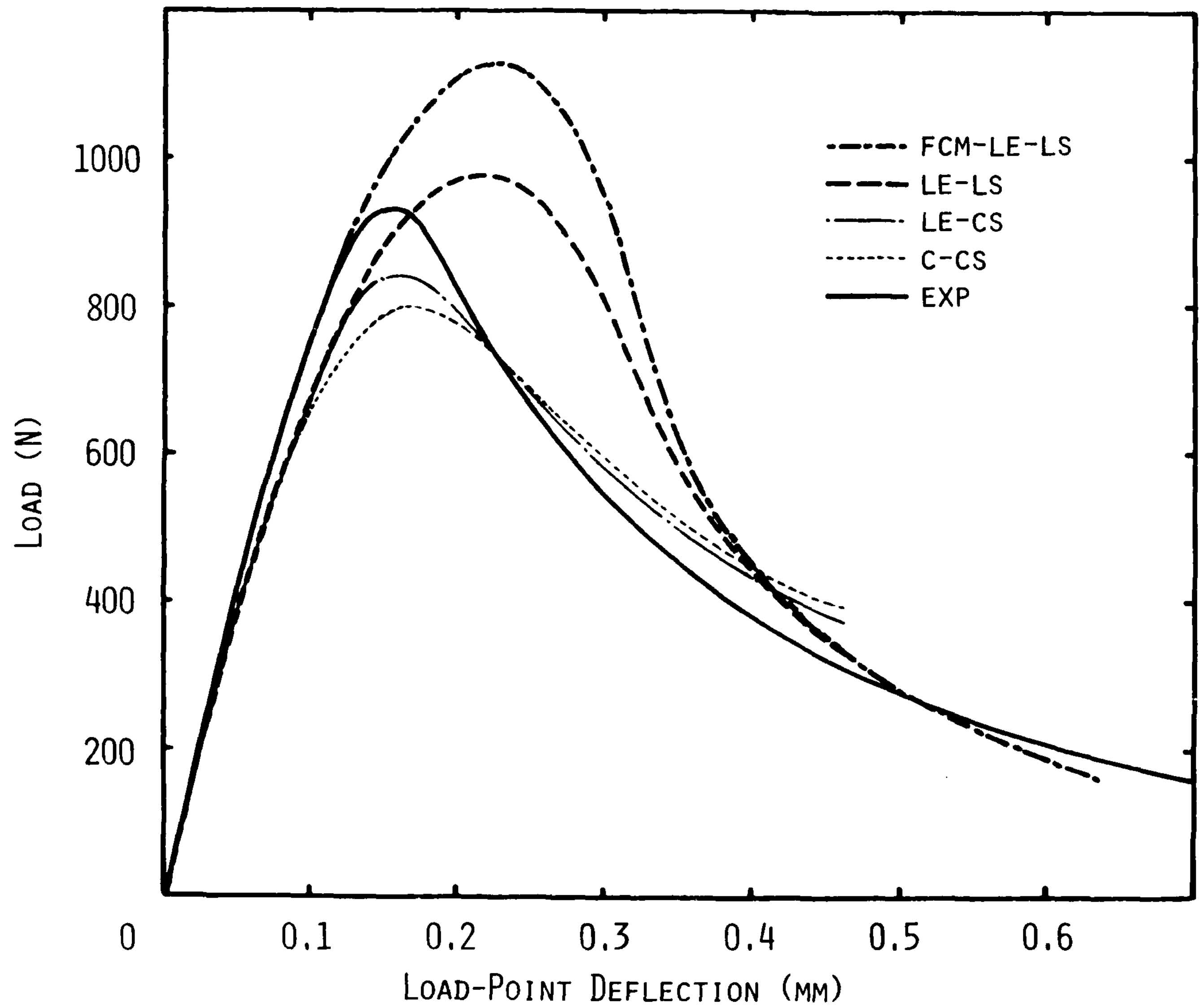

Figure 4. Load versus load-point deflection plots, 2-D model.

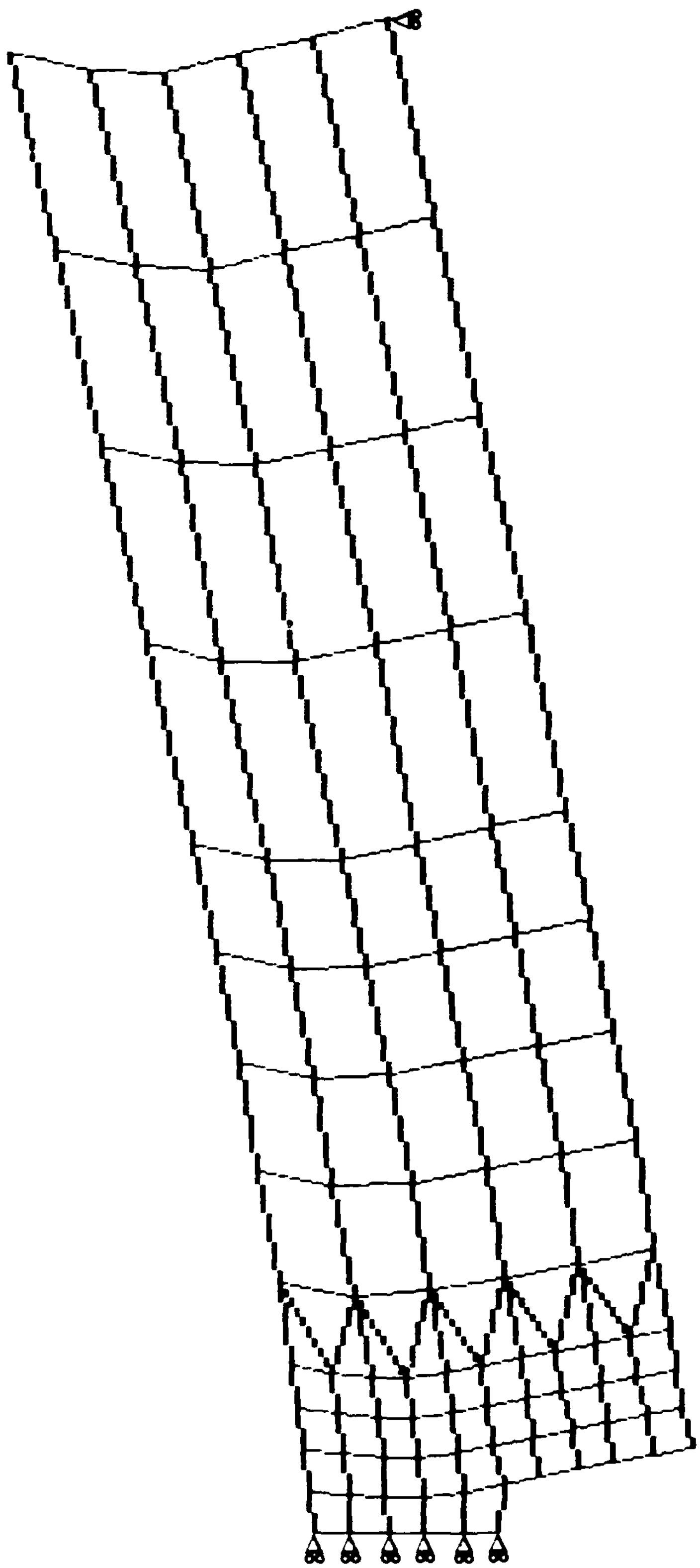

Figure 5. Deformed shape at peak load.

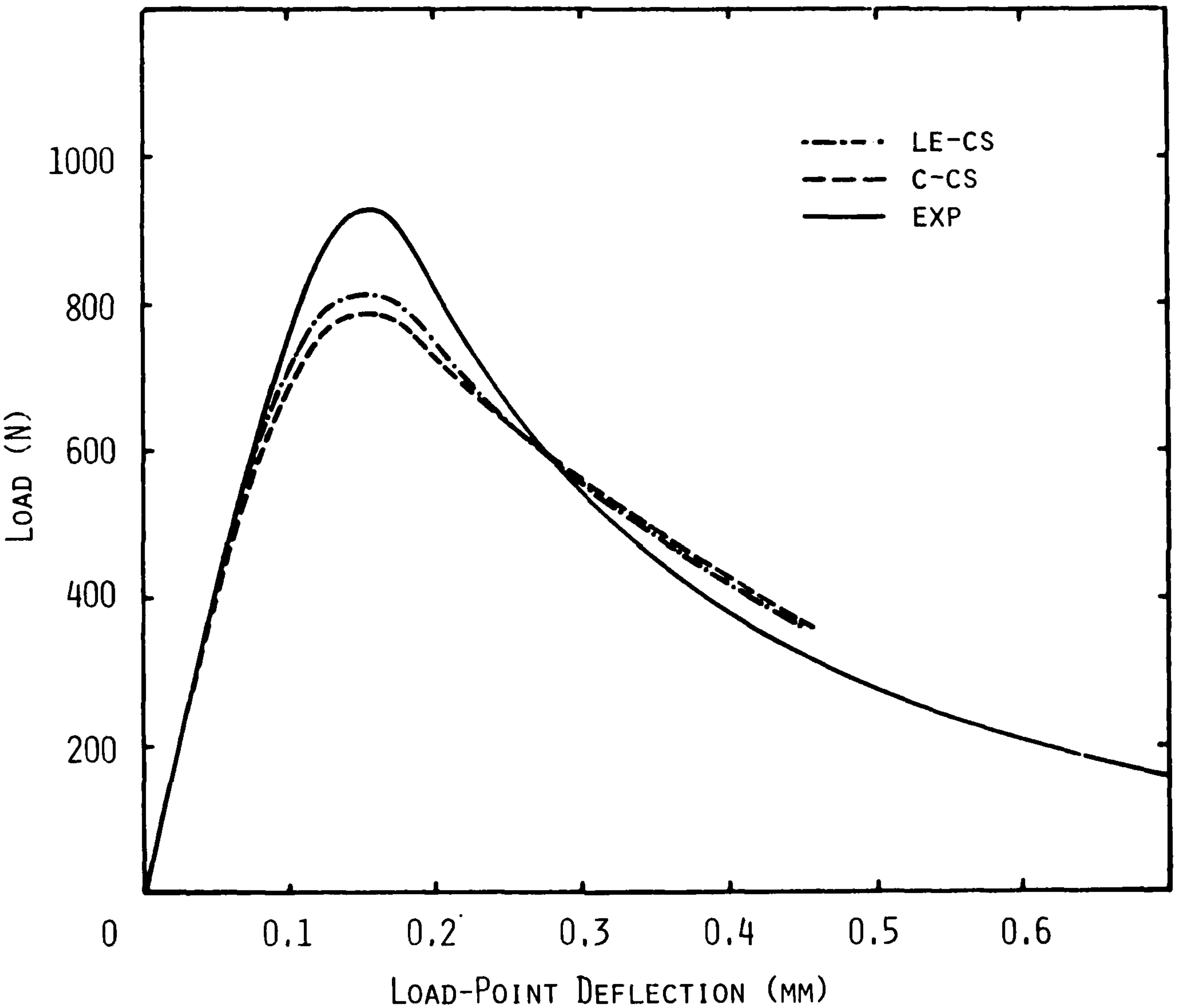

Figure 6. Load versus load-point deflection plots, 3-D model.

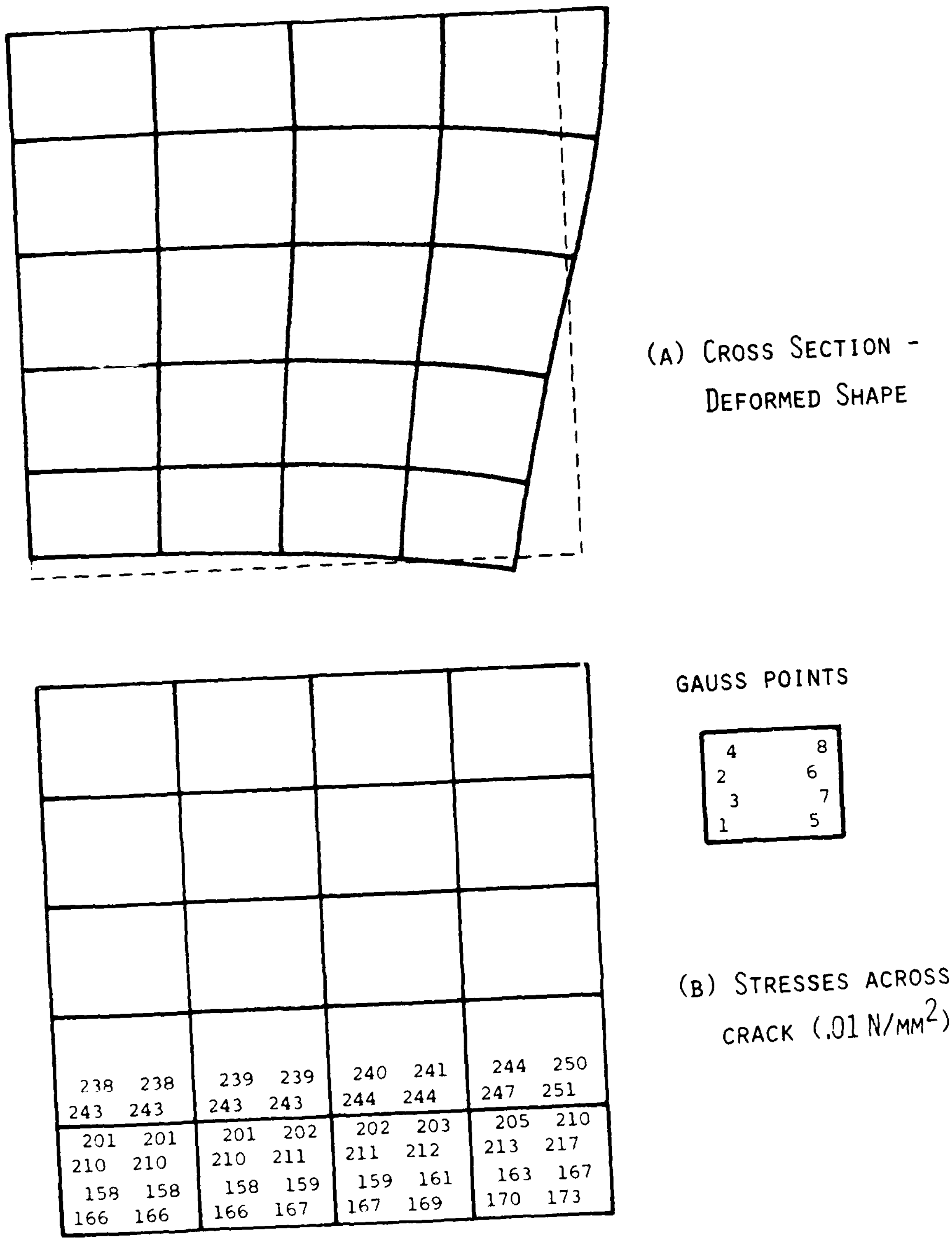

Figure 7. Fracture zone at peak load.

PART 2. SHEAR TRANSFER

INTRODUCTION

To model shear transfer across a crack, an adequate formulation of the constitutive relations representing the transferred stresses is needed. Shear transfer yields successive crack planes which need not be orthogonal to each other. Tensorial invariance is then addressed for the case of orthotropic models. Finally, as it happens in the case of tensile stress transfer, "snap-back" and instability may occur.

SHEAR TRANSFER

Cracks in reinforced concrete are able to transmit large shear forces. Traditionally this transfer has been neglected because of complexity and justified on the assumption that this would be a conservative simplification. In some cases this argument is erroneous (Ref 18 and 19). If a shear slip occurs along the crack, the crack will tend to dilate. If the crack dilatancy is prevented, forces normal to the crack faces will appear. These will have to be compensated by tensile forces on the reinforcement across the crack, increasing the potential for failure.

Shear stresses can be transferred across a crack in three different ways: (1) by aggregate interlock as a result of the roughness of the crack faces, (2) by dowel action or shear resistance of the reinforcement across the crack, (3) by the axial tensile force component in the reinforcement oblique to the plane of cracking.

For members with low reinforcement and for small crack widths, aggregate interlock is the main mechanism of shear transfer. Tests carried out on beams without web reinforcement showed that aggregate interlock accounted for up to 75% of the shear transfer (Ref 20). Hence most attention will be given to this first mechanism of transfer.

EXPERIMENTAL BACKGROUND

Numerous tests have been conducted to evaluate the contribution of each mechanism of shear transfer. To assess transfer by aggregate interlock, shear displacements were imposed on concrete specimens with a single crack. The crack width was maintained constant using a variable external constraint (Ref 20, 21, and 22), or unconstrained and monitored (Ref 23 through 26). In other cases the external constraining force was maintained constant (Ref 27 and 28). To eliminate the effect of dowel action, the concrete specimens were unreinforced (Ref 20) or had the reinforcement through oversized ducts next to the crack (Ref 23 through 26).

Most test results are presented as families of curves relating transferred shear stress to shear slip where each curve corresponds to a crack width (Figure 8). The shear stress is a function of shear slip and crack width (and, indirectly, of the normal stress).

ANALYTICAL BACKGROUND

In the early attemps at modeling shear transfer in finite element methods, the shear stiffness of a cracked element was taken as:

$$G_c = \beta G$$

where G is the shear stiffness of the uncracked element and β is called the shear stiffness reduction factor. This was implemented in ADINA. This model does not reflect the decrease in shear transfer capability when the crack width increases. Shear transfer eventually vanishes as the crack width approaches the aggregate size.

To overcome this difficulty, β has been linked to the crack width (Ref 29 through 32). For instance Cedolin and Dei Poli (Ref 30) used:

$$G_c = G\left(1 - \frac{\varepsilon}{\varepsilon_c}\right) \quad \text{for } 0<\varepsilon<\varepsilon_c$$

$$G_c = 0 \qquad \text{for } \varepsilon>\varepsilon_c$$

where

ε = strain normal to the crack

ε_c = value of ε after which there is no aggregate interlock

When the crack width is kept constant and the shear slip is increased, shear stress increases to a plateau independent of slip (Figure 8). Two analytical models which represent the nonlinear relationships between shear stress and slip are the Rough Crack Model of Bazant and Gambarova (Ref 19), and the Two-Phase Model of Walraven and Reinhardt (Ref 23 and 24). Both models will be more consistent with experimental behavior since they include general anisotropic properties.

THE ROUGH CRACK MODEL

The constitutive laws of the Rough Crack Model were simplified in Reference 33 as:

$$\sigma_{nn} = a_1 a_2 \frac{r}{(1+r^2)^{0.25}} \sqrt{\delta_n \sigma_{nt}}$$

$$\sigma_{nt} = \tau_o \left(1-\sqrt{\frac{2\delta_n}{d_a}}\right) r \frac{a_3 + a_4|r|^3}{1 + a_4 r^4}$$

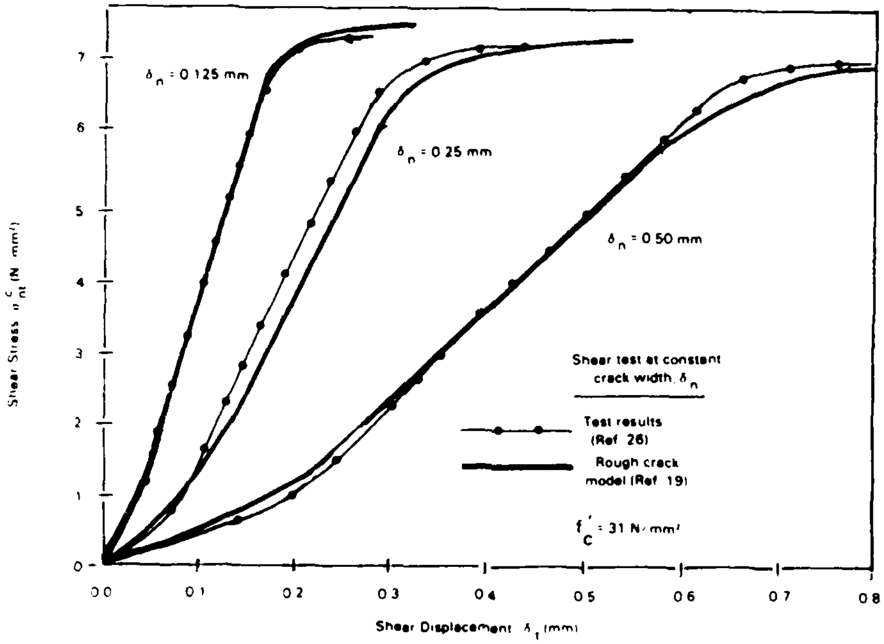

Figure 8. Shear stress versus shear slip.

in which δ_n = crack opening ($\delta_n \leq 0$)

δ_t = relative slip

σ_{nn} = interface normal stress

σ_{nt} = interface shear stress

$r = \delta_t/\delta_n$

$a_1 a_2 = 0.62$

$a_3 = 2.45/\tau_o$

$a_4 = 2.4(1-4/\tau_o)$

$\tau_o = 0.25\, f'_c$

These are empirical expressions based on Paulay and Loeber's tests results (Ref 26). The following assumptions were made:

- σ_{nn} is always compressive
- for $\delta_t = 0$ and $\delta_n > 0$ the crack faces cannot be in contact and therefore $\sigma_{nn} = 0$
- if $\delta_n = 0$ there is no crack and $\delta_t \neq 0$ cannot be obtained. Hence $\delta_t \to 0$ when $\delta_n \to 0$.

- for constant δ_t and increasing δ_n, both $|\sigma_{nn}|$ and $|\sigma_{nt}|$ decrease

As a consequence, if B is the crack stiffness matrix defined by

$$b_{ij} = \frac{\delta|\sigma_i|}{\delta\ \delta_j} \qquad \text{with } i = nn,nt \quad j = n,t$$

B is never positive definite which can cause numerical problems in finite element programs.

IMPLEMENTATION IN ADINA

The transfer of tensile stresses across a crack with a smeared crack approach and tension softening behavior resulted in a negative stiffness for the cracked element and was implemented using a residual load vector to redistribute the stresses during equilibrium iterations (Ref 1). This approach could also be followed to include the transfer of shear stresses by combining the Rough Crack Model and the Crack Band Model, discussed in Part 1. A similar approach for mixed-mode crack propagation appeared in Reference 34.

PRINCIPAL AXES ROTATION

In finite element implementations, cracking at a point occurs when one of the principal stresses reaches the tensile strength. A failure or cracking plane is defined upon cracking. Most computer programs, including ADINA, keep this plane constant and only allow successive planes to form perpendicular to the first one and to each other. However, when shear stress transfer across the crack is allowed, successive crack planes will generally not be perpendicular to each other (Ref 17).

In order to address this inconsistency, several recent approaches have been proposed, which are discussed below.

The Rotating Crack Model

It is assumed in the rotating crack model that the cracks are formed normal to the major principal tensile strain and rotate with it. Experiments carried out by Vecchio and Collins (Ref 35) on square, reinforced concrete panel sections support the assumption that the main crack formation is normal to the major principal tensile strain.

Cope et al. (Ref 36), first applied a rotating crack model, using a set of perpendicular axes, which followed the tensile strain rotation in a step-wise fashion. Gupta and Akbar (Ref 37) improved the model by considering a single crack which followed the tensile strain rotation in a continuous fashion. This method has been used by several researchers (Ref 38 through 41); however, the rotating crack model has been criticized (Ref 9, 42, and 43) for neglecting the previously formed cracks.

The Multiple Crack Model

An alternative approach to the rotating crack model was formulated by De Borst and Nauta (Ref 43, 44, and 45) and independently by Riggs and Powell (Ref 46), following the original development by Litton (Ref 47). They assumed that multiple, nonorthogonal cracks can form at an integration point. In this procedure the total strain increment is first decomposed into a solid concrete strain increment and a crack strain increment. Then, crack shear and normal strains are related to the corresponding stresses and an incremental crack stress-strain matrix is derived. In a similar fashion a solid concrete stress-strain matrix is formed. Finally, matrices of all cracks are assembled and an expression for the total stress-strain matrix is obtained.

The multiple crack model leads to excessive formation of new cracks, which led to the adoption of a threshold angle that allows new cracks to form only after the rotation of principal stresses reaches that angle (Ref 43). Numerical difficulties also are encountered because the crack stress-strain matrices are not positive definite.

ORTHOTROPIC VERSUS ANISOTROPIC MODELS

Numerous finite element analyses have been conducted using incrementally linear constitutive equations characterized by an orthotropic tangential stiffness. In the stress-free state isotropy is assumed and is replaced by stress-induced orthotropy when the tensile stress reaches the tensile strength. This scheme is also used in ADINA. In cases where the principal stresses rotate during the loading history, this model is not tensorially invariant; i.e., the predicted response is affected by the initial choice of axes (Ref 9). Dilatancy of the crack cannot be represented when orthotropy is assumed. Orthotropy assumes no relation between the shear strains and normal stresses. Invariance is maintained if general stress-induced anisotropy is assumed instead (Ref 9). An empirical anisotropic tangential stiffness matrix, such as the one derived from the Rough Crack Model, would be more suitable.

SNAP-BACK AND INSTABILITY

A general load-deflection response demonstrating the snap-back phenomenon is shown in Figure 9 (Ref 48). If load control were attempted to obtain this response, the path ABDEJ would be obtained since load control assumes a monotonic increment of the load. On the other hand, displacement control would yield a more complete response following the path ABCDEFHI. In either case the segment FGH representing the snap-back phenomenon could not be obtained since displacement is incremented monotonically.

To overcome the difficulty in obtaining a complete response, Riks (Ref 49) and Crisfield (Ref 41, 48, and 50) developed a procedure, known as Riks' or arc-length method, using a constraint equation fixing the step size in the load/deflection space.

Snap-back may occur in practice when strain softening is considered. Two simple examples are shown in References 41 and 51 for a bar in tension:

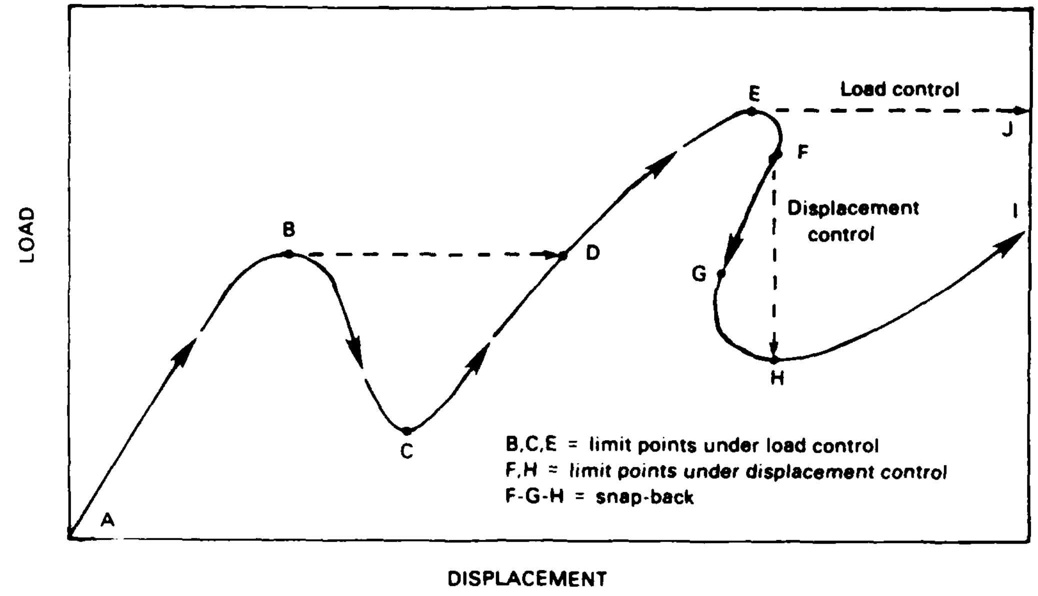

Figure 9. Snap-back phenomenon.

For a stress-strain law given by

$$\sigma = E\varepsilon \qquad \text{if } \varepsilon<\varepsilon_e \qquad \text{with } \varepsilon_e = f_t/E$$

$$\sigma = f_t\,[1-(\varepsilon-\varepsilon_e)] \qquad \text{if } \varepsilon_e<\varepsilon<\varepsilon_u \qquad \text{with } \varepsilon_u = n\varepsilon_e$$

$$\sigma = 0 \qquad \text{if } \varepsilon>\varepsilon_u$$

where the bar is composed of m square elements in which one of the elements is strain softening and the other (m-1) unloading, the bar will have an average strain increment of

$$\varepsilon = \frac{1}{m}\left[-(m-1)\frac{\Delta\sigma}{E} + \frac{\Delta\sigma}{E/(n-1)}\right] = \left[\frac{n}{m} - 1\right]\frac{\Delta\sigma}{E}$$

It is observed that for m>n the average strain in the post-peak regime is smaller than the peak load strain ε_e; thus, a snap-back is orginated. Riks' method has been implemented in ADINA (Ref 52) and applied to concrete cracking (Ref 41, 48, 49, and 53).

PART 3. BOND-SLIP

INTRODUCTION

In finite element analysis of reinforced concrete, bond-slip between reinforcement and concrete has been modeled using interface elements. Interface elements often use empirical, nonlinear bond stress-slip relationships.

INTERFACE ELEMENTS

The simplest interface element is the bond-link element developed by Ngo and Scordelis (Ref 54). This is a dimensionless element which connects two nodes with identical coordinates. It can be viewed as consisting of two orthogonal springs between the two nodes. De Groot et al. (Ref 55), generated a more complex element by combining the reinforcement and adjacent concrete into a finite bond-zone element. Hoshino (Ref 56) and Schafer (Ref 57) developed the dimensionless contact element, which gives a continuous connection between two elements. A comparison between these different models (Ref 58) showed that best results are obtained using contact elements with quadratic or higher order displacement functions.

An isoparametric contact element has been developed by Keuser, Mehlhorn et al. (Ref 59, 60, and 61), which is compatible with the two- and three-dimensional elements of ADINA. This contact element has been programmed in a modular structure to facilitate the input of user-supplied bond stress-slip relationship data.

BOND MECHANISMS

The mechanism of bond comprises three main components: chemical adhesion, friction, and mechanical interlock between bar ribs and concrete. Initially, for very small values of bond stress of up to 1 N/mm^2 chemical adhesion is the only resisting mechanism (Ref 62). If the bond stress is increased, chemical adhesion is destroyed and replaced by the wedging action of the ribs. This wedging action originates secondary internal radial cracks (Ref 63), longitudinal cracks, and crushing in front of the ribs. If inadequate confinement is provided, bond failure would occur as soon as the cracks spread across the concrete cover of the bar. With proper confinement, the bond stress reaches a maximum near $f'_c/3$ before decreasing as the concrete between ribs fails in shear and a frictional type of behavior ensues as shown in (Figure 10) (Ref 62).

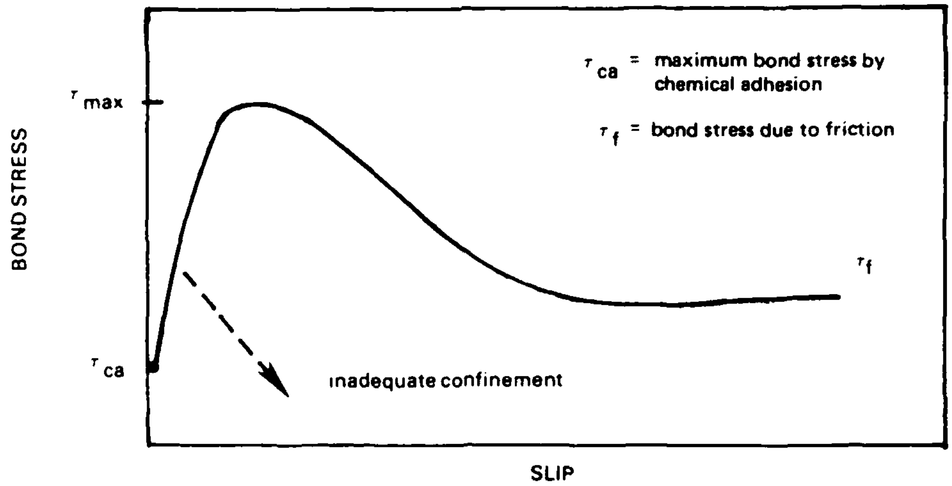

Figure 10. Typical bond-slip relationship.

EMPIRICAL BOND-SLIP RELATIONSHIPS

In order to obtain local bond stress-slip relationships for finite element modeling, the force to pull short lengths of embedded reinforcement out of concrete are measured. For embedment lengths of one to five lug spacings, consistent bond stress-slip relationships similar to the one depicted in Figure 10 have been obtained (Ref 62, 64, and 65). The use of longer embedment lengths leads to a nonuniform distribution of bond stress (Ref 66), difficulty in measuring local values without disturbing them, and different responses if the bar is pulled or pushed (Ref 67).

The parameters influencing bond-slip behavior are: load history, confinement, clear bar spacing, bar size and configuration, concrete strength, transverse pressure and loading rate. Experimental-based, local bond stress-slip relationships have been derived which are adequate for confined and unconfined bars to be used in the finite element methodology (Ref 65).

EFFECT OF BOND ON CRACK PATTERN

Bond-slip based on De Groot's model (Ref 55) has been implemented together with strain softening in the study of fracture of reinforced concrete (Ref 68). The inclusion of bond-slip produces a more realistic crack pattern, which is less diffuse and successfully represents primary and secondary cracking as observed by Goto (Ref 63).

CONCLUSIONS ANu RECOMMENDATIONS

Mode I Fracture

A smeared crack approach has been implemented in ADINA for two and three dimensional nonlinear concrete elements in tension. The experimental results from tests on 12 single-edge notched beams were analyzed and good agreement was found. In particular it was shown that:

- the FCM and CBM approaches yielded similar results

- the bluntness of the crack front affected the model's behavior

- 3-D elements yielded a stiffer response than 2-D elements

- the crack front could be assumed straight.

In this application only mode I fracture occurs, and only tensile stress transfer across the crack needed to be modeled.

Mixed Mode Fracture

Mixed mode fracture including shear stress transfer is the general crack propagation mechanism. A benchmark problem in mixed mode fracture was presented by Arrea and Ingraffea (Figure 11) and studied in References 68 through 72. Initial attempts at modeling the shear transfer using a constant shear retention factor, β, and ADINA yielded results with almost no softening after peak load (Figure 12) and a crack pattern which contrasts with experimental observations (Figure 13). By considering a mode II fracture energy, Rots and De Borst successfully predicted an experimentally verified load-deflection response. However the model's crack pattern at ultimate residual load remained fixed and was inconsistant with physical observations.

It is expected that the consideration of an adequate shear transfer model, such as the Rough Crack Model that includes general anisotropy, will be more consistent with experimental observations and measurements. By considering the crack dilatancy, the initial crack next to the notch tip will tend to open further and propagate in the direction indicated by experiments.

Bond-Slip

It is proposed to update the current version of ADINA with an isoparametric contact element for bond. The versatility of this model will allow for an easy updating of the bond stress-slip relationship. The empirical stress-strain relationship derived by Eligehausen, Popov and Bertero appears most complete and should be implemented in the contact element.

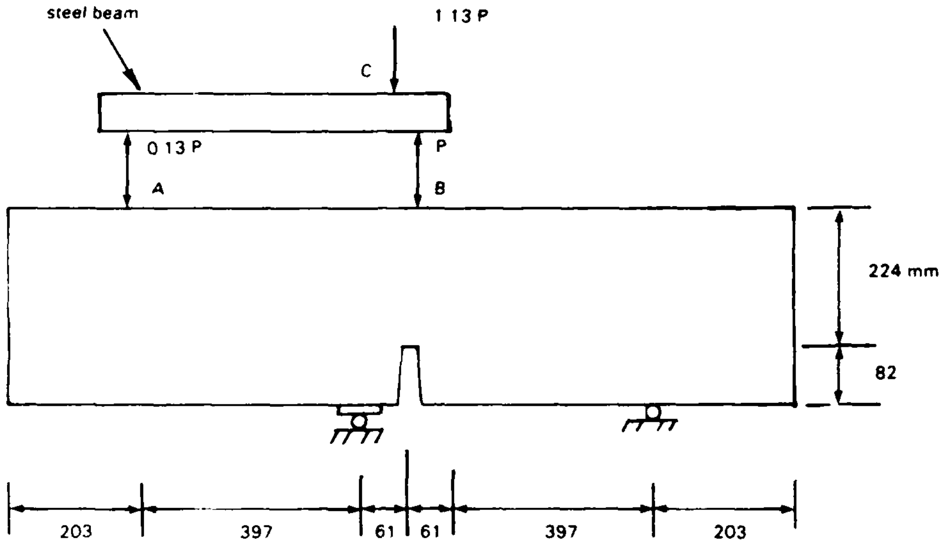

Figure 11. Single notch shear specimen.

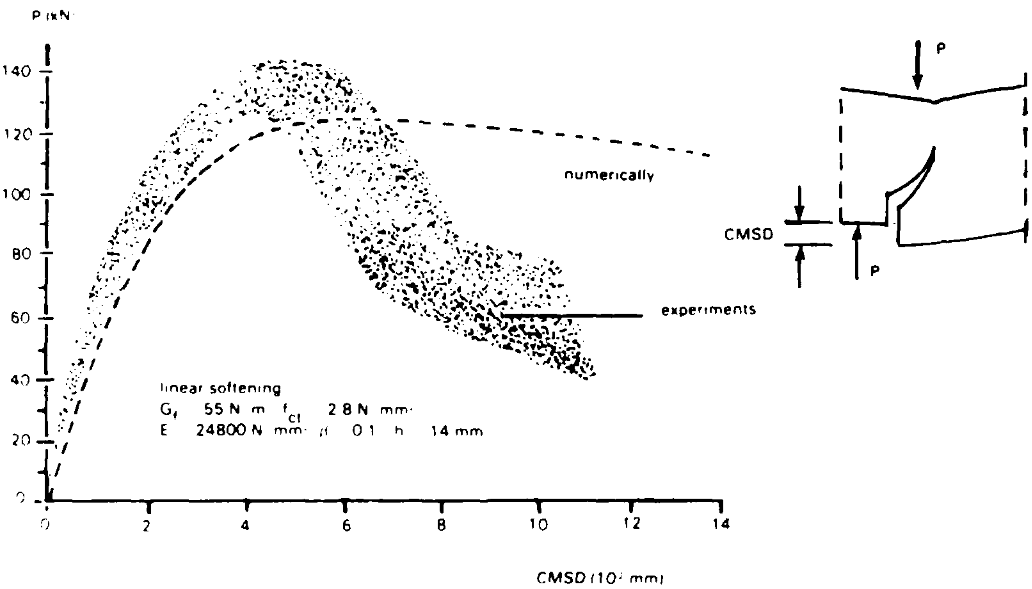

Figure 12. Load versus crack mouth sliding displacement.

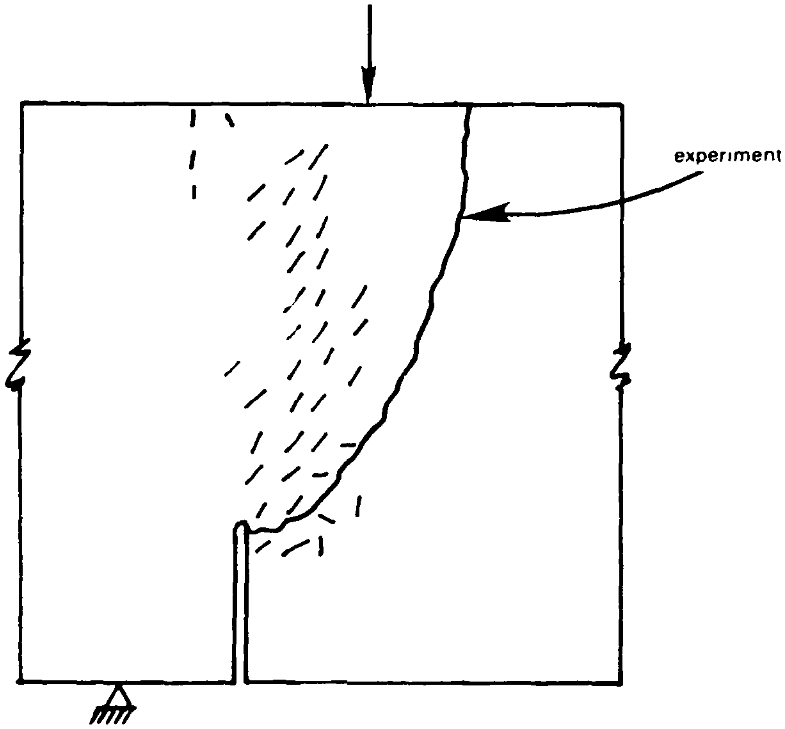

Figure 13. Crack pattern.

REFERENCES

1. Naval Civil Engineering Laboratory. Technical Report R-924: Fracture energy for three point bend tests on single edge notched beams, by L.J. Malvar and G.E. Warren. Port Hueneme, CA, Mar 1988.

2. ADINA Engineering Inc. ADINA: A finite element program for automatic dynamic incremental nonlinear analysis, Watertown, MA, Dec 1985.

3. Y.R. Rashid. "Analysis of prestressed concrete pressure vessels," Nuclear Engineering and Design, vol 7, no. 4, 1968, pp 334-344.

4. Z.P. Bazant and L. Cedolin. "Blunt crack propagation in finite element analysis," American Society of Civil Engineers, Journal of the Engineering Mechanics Division, vol 105, no. EM2, 1979, pp 297-315.

5. ________. "Fracture mechanics of reinforced concrete," American Society of Civil Engineers, Journal of the Engineering Mechanics Division, vol 106, no. EM6, Dec 1980, pp 1287-1306 (discussion by D. Darwin and R. Dodds, vol 108, no. EM2, Apr 1982, pp 464-471).

6. Z.P. Bazant and B.H. Oh. "Crack band theory for fracture of concrete," Materials and Structures, vol 16, no. 93, May-Jun 1983, pp 155-177.

7. Z.P. Bazant, J-K. Kim, and P. Pfeiffer. "Continuum model for progressive cracking and identification of nonlinear fracture parameters," NATO-ARW, Northwestern University, Sep 1984. Applications of Fracture Mechanics to Cementitious Composites (S.P. Shah, editor), Nijhoff Publishers, Dordrecht, The Netherlands, 1985, pp 197-246.

8. A. Hillerborg, M. Modeer, and P.E. Petersson. "Analysis of crack formation and crack growth in concrete by means of fracture mechanics and finite elements," *Cement and Concrete Research*, vol 6, 1976, pp 773-782.

9. Z.P. Bazant. "Comment on orthotropic models for concrete and geomaterials," American Society of Civil Engineers, Journal of Engineering Mechanics, vol 109, no. 3, Jun 1983.

10. H.A.W. Cornelissen, D.A. Hordijk, and H.W. Reinhardt. "Experiments and theory for the application of fracture mechanics to normal and lightweight concrete," *in Proceedings of the International Conference on* Fracture Mechanics of Concrete, Lausanne, Oct 1985. Fracture Toughness and Fracture Energy of Concrete, Elsevier Science Publishers, Amsterdam, 1986, pp 565- 575.

11. G. Valente. "Size effect on measured fracture energy of concrete in three point bend tests on notched beams," in Proceedings of the Fourth International Conference, Numerical Methods in Fracture Mechanics, San Antonio, TX, Mar 1987, pp 433- 447.

12. J.G. Rots, G.M.A. Kusters, and J. Blaauwendraad. "Strain softening simulations of mixed mode concrete fracture," in Proceedings of the SEM-RILEM International Conference, Fracture of Concrete and Rock, Houston, TX, Jun 1987.

13. Lund Institute of Technology. Report TVBM-1006: Crack growth and development of fracture zones in plain concrete and similar materials, by P.E. Petersson, Division of Building Materials, S-221 00, Lund, Sweden, 1981.

14. H.W. Reinhardt. "Fracture mechanics of an elastic softening material like concrete," HERON, vol 29, no. 2, 1984.

15. M. Suidan and W.C. Schnobrich. "Finite element analysis of reinforced concrete," American Society of Civil Engineers, Journal of the Structural Division, vol 99, no. STIO, Oct 1973.

16. W.C. Schnobrich, M.H. Salem, D.A. Pecknold, and B. Mohraz. Discussion of "Nonlinear stress analysis of reinforced concrete," by S. Valliapan and T.F. Doolan, American Society of Civil Engineers, Journal of the Stuctural Division, vol 98, no. STIO, 1972, pp 2327-2328.

17. American Society of Civil Engineers. State-of-the-art report: Finite Element Analysis of Reinforced Concrete, Task Committee on Finite Element Analysis of Reinforced Concrete Structures, 1982.

18. Z.P. Bazant and T. Tsubaki. "Optimum slip-free limit design of concrete reinforcing nets," American Society of Civil Engineers, Journal of the Structural Division, vol 105, no. ST2, Feb 1979, pp 327-346.

19. Z.P. Bazant and P. Gambarova. "Rough cracks in reinforced concrete," American Society of Civil Enginers, Journal of the Structural Division, vol 106, no. ST4, Apr 1980, pp 819-843.

20. R.C. Fenwick and T. Paulay. "Mechanisms of shear resistance in concrete beams," American Society of Civil Engineers, Journal of the Structural Division, vol 94, no. STIO, Oct 1968, pp 2325-2350.

21. T. Paulay and P.J. Loeber. "Shear transfer by aggregate interlock," Special Publication SP42, American Concrete Institute, 1974, pp 1-15.

22. J. Houde and M.S. Mirza. "Investigation of shear transfer across cracks by aggregate interlock," Research Report No. 72-06, Departement de Genie Civil, Division de Structures, Ecole Polytechnique de Montreal, Montreal, Canada, 1972.

23. S.G. Millard and R.P. Johnson. "Shear transfer across cracks in reinforced concrete due to aggregate interlock and dowel action," Magazine of Concrete Research, vol 36, no. 126, Mar 1984, pp 9-21.

24. __________. "Shear transfer in cracked reinforced concrete," Magazine of Concrete Research, vol 37, no. 130, Mar 1985, pp 3-15.

25. J.C. Walraven and H.W. Reinhardt. "Theory and experimentation on the mechanical behavior of cracks in plain and reinforced concrete subjected to shear loading," HERON, vol 26, no. IA, 1981, 68 p.

26. __________. "Crack in concrete subject to shear," American Society of Civil Engineers, Journal of the Structural Division, vol 108, no. STI, Jan 1982, pp 207-224.

27. A.H. Mattock. "Shear transfer in concrete having reinforcement at an angle to the shear plane," Special Publication SP42, American Concrete Institute, 1974, pp 17-42.

28. A.H. Mattock and N.M. Hawkins. "Shear transfer in reinforced concrete - recent research," Journal of Prestressed Concrete Institute, vol 17, no. 2, Mar-Apr 1972.

29. P.C. Perdikaris and R. White. "Shear modulus of precracked R/C panels," American Society of Civil Engineers, Journal of Structural Engineering, vol 111, no. 2, Feb 1985, pp 270-289.

30. L. Cedolin and S. Dei Poli. "Finite element studies of shear critical R/C beams," American Society of Civil Engineers, Journal of the Engineering Mechanics Division, vol 103, no. EM3, Jun 1977, pp 395-410.

31. R.S.H. Al-Mahaidi. "Nonlinear finite element analysis of reinforced concrete deep members," Report 79-1, Department of Structural Engineering, Cornell University, Ithaca, NY, Jan 1979.

32. J.S. Gedling, N.S. Mistry, and A.K. Welch. "Evaluation of material models for reinforced concrete structures," Computers and Structures, vol 24, no. 2, 1986, pp 225-232.

33. S. Dei Poli, P.G. Gambarova, and C. Karakoc. "Aggregate interlock role in R/C thin webbed beams in shear," American Society of Civil Engineers, Journal of Structural Engineering, vol 113, no. 1, Jan 1987, pp 1-19.

34. D.J.W. Wium, O. Buyukozturk, and V.C. Li. "Hybrid model for discrete cracks in concrete," American Society of Civil Engineers, Journal of Engineering Mechanics, vol 110, no. 8, Aug 1984, pp 1211-1229.

35. F. Vecchio and M.P. Collins. "The response of reinforced concrete to inplane shear and normal stresses," ISBN0-7727-7029- 8, Publication No. 82-03, University of Toronto, Toronto, Ontario, 1982.

36. R.J. Cope, P.V. Rao, L.A. Clark, and P. Norris. "Modelling of reinforced concrete behavior for finite element analysis of bridge slabs," vol 1, Numerical Methods for Non-Linear Problems (C. Taylor et al., eds.), 1980, pp 457-470.

37. A.K. Gupta and H. Akbar. "Cracking in reinforced concrete analysis," American Society of Civil Engineers, Journal of Structural Engineering, vol 110, no. 8, Aug 1984, pp 1735-1746.

38. L.G. Nilsson and M. Oldenbug. "On the numerical simulation of tensile tests," Finite Element Methods for Nonlinear Problems, Proceedings of the Europe-US Symposium, Norwegian Institute of Technology, Trondheim, Norway, Aug 1985, pp 103-117.

39. R.V. Milford and W.C. Schnobrich. "Numerical model for cracked reinforced concrete," in Proceedings of the International Conference on Computer Aided Analysis and Design of Concrete Structures, Split, Yugoslavia, Sep 1984, pp 71-84.

40. ________. "The application of the rotating crack model to the analysis of reinforced concrete shells" Computational Strategies for Nonlinear and Fracture Mechanics Problems, Computers and Structures, vol 20, no. 1-3, 1985, pp 225-234.

41. M.A. Crisfield. "Difficulties with current numerical models for reinforced concrete and some tentative solutions," in Proceedings of the International Conference on Computer Aided Analysis and Design of Concrete Structures, Split, Yugoslavia, Sep 1984, pp 331-357.

42. Z.P. Bazant. Discussion on Session 2, Structural Modelling for Numerical Analysis, Final Report IABSE Colloquium on Advanced Mechanics of Reinforced Concrete, Delft University Press, Delft, Holland, 1981.

43. R. de Borst and P. Nauta. "Non-orthogonal cracks in a smeared finite element model," Engineering Computations, vol 2, Mar 1985, pp 35-46.

44. ________. "Smeared crack analysis of reinforced concrete beams and slabs failing in shear," in Proceedings of the International Conference on Computer Aided Analysis and Design of Concrete Structures, Split, Yugoslavia, Sep 1984, pp 261-273.

45. R. de Borst. "Smeared cracking, plasticity, creep and thermal loading - a unified approach," Computer Methods in Applied Mechanics and Engineering, vol 62, 1987, pp 89-110.

46. H.R. Riggs and G.H. Powell. "Rough crack model for analysis of concrete," American Society of Civil Engineers, Journal of Engineering Mechanics, vol 112, no. 5, May 1986, pp 448-464.

47. R.W.A. Litton. A contribution to the analysis of concrete structures under cyclic loading, Dissertation, University of California, Berkeley, CA, 1976.

48. M.A. Crisfield. "A fast incremental/iterative solution procedure that handles snap-through," Computers and Structures, vol 13, 1981, pp 55-62.

49. E. Riks. "An incremental approach to the solution of snapping and buckling problems," International Journal of Solids and Structures, vol 15, 1979, pp 524-551.

50. M.A. Crisfield and J. Wills. "Solution strategies and softening materials," Computer Methods in Applied Mechanics and Engineering, vol 66, 1988, pp 267-289.

51. R. de Borst. "Computation of post-bifurcation and post-failure behavior of strain-softening solids," Computers and Structures, vol 25, no. 2, 1987, pp 211-224.

52. K.J. Bathe and E.N. Dvorkin. "On the automatic solution of nonlinear finite element equations," Computers and Structures, vol 17, no. 5/6, 1983, pp 871-879.

53. R. de Borst. "Application of advanced solution techniques to concrete cracking and non-associated plasticity," Numerical Methods for Non-Linear Problems, vol 2 (C.Taylor et al., eds.), Apr 1984, pp 314-325.

54. D. Ngo and A.C. Scordelis. "Finite element analysis of reinforced concrete beams," Journal of the American Concrete Institute, 1967, pp 152-163.

55. A.K. de Groot, G.M.A. Kusters, and T. Monnier. "Numerical modelling of bond-slip behavior," HERON, vol 26, no. IB, 1981, 90 p.

56. M. Hoshino. Ein Beitrag zur Untersuchung des Spannungszustandes an Arbeitsfugen mit Spannglied-Kopplungen von abschnittweise in Ortbeton hergestellten Spannbetonbruecken, Dissertation, Technische Hochschule, Schale, Darmstadt, Germany, 1974.

57. H. Schafer. "A contribution to the solution of contact problems with the aid of bond elements," Computer Methods in Applied Mechanics and Engineering, vol 6, 1975, pp 335-354.

58. M. Keuser and G. Mehlhorn. "Finite element models for bond problems," American Society of Civil Engineers, Journal of Structural Engineering, vol 113, no. 10, Oct 1987, pp 2160-2173.

59. M. Keuser, G. Mehlhorn, and V. Cornelius. "Bond between prestressed steel and concrete - computer analysis using ADINA," Computers and Structures, vol 17, no. 5/6, 1983, pp 669-676.

60. G. Mehlhorn, J. Kollegger, M. Keuser, and W. Kolmar. "Nonlinear contact problems - a finite element approach implemented in ADINA," Computers and Structures, vol 21, no. 1/2, 1985, pp 69-80.

61. G. Mehlhorn and M. Keuser. "Isoparametric contact elements for analysis of reinforced concrete," American Society of Civil Engineers, Finite Element Analysis of Reinforced Concrete Structures, Proceedings of a seminar sponsored by the Japan Society for the Promotion of Science and the US National Science Foundation, Tokyo, Japan, 1985, pp 329-347.

62. P. Gambarova and C. Karakoc. "Shear confinement interaction at the bar to concrete interface," Bond in Concrete, Proceedings of the International Conference held at Peisley College of Technology, Scotland, UK, 1982, pp 82-96 (Applied Science Publishers, P. Bartos, editor).

63. Y. Goto. "Cracks formed in concrete around deformed tension bars," Journal of the American Concrete Institute, no. 4, 1971.

64. N.M. Hawkins, I.J. Lin, and F.L. Jeang. "Local bond strength of concrete for cyclic reversed loading," Bond in Concrete, Proceedings of the International Conference held at Peisley College of Technology, Scotland, UK, 1982, pp 151-161 (Applied Science Publishers, P. Bartos, editor).

65. R. Eligehausen, E.P. Popov, and V.V. Bertero. "Local bond stress-slip relationships of deformed bars under generalized excitations," Report UCB/EERC-83/23, University of California, Berkeley, CA, 1983, 169 pp.

66. A.H. Nilson. "Internal measurement of bond slip," Proceedings, Journal of the American Concrete Institute, vol 69, no. 7, Jul 1972, pp 439-441.

67. A.D. Cowell, E.P. Popov, and V.V. Bertero. "Effects of concrete types and loading conditions on local bond-slip relationships," Report UCB/EERC-82/17, University of California, Berkeley, CA, 1982, 62 pp.

68. RILEM Technical Committee 90-FMA. "Fracture mechanics of concrete/ applications," Second Draft Report over the State-of-the-Art, Division of Structural Engineering, Lulea University of Technology, S-951 87 Lulea, Sweden.

69. M. Arrea and A.R. Ingraffea. "Mixed-mode crack propagation in mortar and concrete," Report No. 81-13, Department of Structural Engineering, Cornell University, Ithaca, NY, 143 pp.

70. J.G. Rots, P. Nauta, G.M.A. Kusters, and J. Blaauwendraad. "Smeared crack approach and fracture localization in concrete," HERON, vol 30, no. 1, 1985, 48 pp.

71. J.G. Rots and R. de Borst. "Analysis of mixed-mode fracture in concrete," American Society of Civil Engineers, Journal of Engineering Mechanics, vol 113, no. 11, Nov 1987, pp 1739-1758.

72. Concrete Mechanics, Cooperative Research between Institutions in the Netherlands and the USA. Third Meeting at Delft University of Technology, Delft, Holland, Jun 1983 (P. Gergely and R.N. White, Cornell University, J.W. Frenay and H.W. Reinhardt, Delft University, editors).

Appendix A

FICTITIOUS CRACK MODEL

In the Fictitious Crack Model, crack propagation is accomplished by releasing successive nodes and inserting a residual force between them that is a function of the crack opening. In this example, nodes 7 to 21 are released. Since these nodes belong to the axis of symmetry of the specimen the coding is simplified. A bilinear strain softening is used.

<u>CHANGES IN IUSER.F77</u>

```
C*I     * * *     I N S E R T     U S E R - S U P P L I E D     C O D I N G  IUSER 58
C*I                                                                          IUSER 59
C*I     * * *     T O     S E T     M F L A G                                IUSER 60
C*I                                                                          IUSER 61
C*I                                                                          IUSER 62
      DO 100 I=7,21
      IF (M .EQ. I) MFLAG = 1
  100 CONTINUE
      RETURN                                                                 IUSER 63
C*I                                                                          IUSER 64
```

<u>CHANGES IN USERSL.F77</u>

```
C*I     * * *     I N S E R T     U S E R - S U P P L I E D     C O D I N G  USERS109
C*I                                                                          USERS110
C*I                                                                          USERS111
      XWC = DD(2)*2.0
      IF (XWC . LE. 0.0) THEN
      RR(2) = 0.0
        ELSE IF (XWC .LE. 0.01840) THEN
        RR(2) = -500.0*(4.2-182.56*XWC)
        ELSE IF (XWC .LE. 0.09202) THEN
        RR(2) = -500.0*(1.05-11.41*XWC)
        ELSE
        RR(2) = 0.0
      END IF
      WRITE (6,*) 'M,DD(2),RR(2)',M,DD(2),RR(2)
      RETURN                                                                 USERS112
C*I                                                                          USERS113
C*FILE END                                                                   USERS114
      END                                                                    USERS115
```

Appendix B

CRACK BAND MODEL, TWO-DIMENSIONAL

To implement a smeared crack approach, additional data has to be read by the program. The user must provide an additional card (2-D solid elements, material 5, card d) where the choice of softening is indicated, as well as band width, soft element width (usually same as band width), fracture energy and maximum aggregate size (format I5,4F10.0). The dimension of the vector CRKSTR is increased to memorize the unloading point from the virgin curve.

<u>CHANGES IN TODMFE.F77</u>

```
     1      IDWAS/ 0, 0, 0,18,18, 0,10,15,15,33,33, 0, 0,26,6*0/,        TODMFE93

      COMMON /SOFT/ ISCODE,WWCC,ELWW,GGFF,DDAA                           TDFE  42

      IF (MODEL.EQ.5) READ(IIN,1005) ISCODE,WWCC,ELWW,GGFF,DDAA          TDFE 101

 1005 FORMAT (I5,4F10.0)                                                 TDFE1219

      COMMON /SOFT/ ISCODE,WWCC,ELWW,GGFF,DDAA                           MATRT214

      WRITE (6,2239) ISCODE,WWCC,ELWW,GGFF,DDAA                          MATRT244

 2239 FORMAT(/38H (BB) CODE FOR TENSILE STRESS TRANSFER,I5,              MATRT726
     1       /38H      1=LINEAR SOFTENING            ,
     2       /38H      2=CORNELISSEN'S SOFTENING     ,
     3       /38H     SOFT BAND WIDTH (WWCC)         ,F10.5,
     4       /38H     SOFT ELEMENT WIDTH (ELWW)      ,F10.5,
     5       /38H     FRACTURE ENERGY (GGFF)         ,F10.8,
     6       /38H     MAXIMUM AGGREGATE SIZE (DDAA)  ,F10.5)
```

<u>CHANGES IN ELT2D4.F77</u>

```
      IDW=18*ITWO                                                        ELT2D438

      DIMENSION PROP(1),WA(18,1),YZ(1),NOD5(1),NODS(1),TEMPV1(1)         ICDMOD16

      DO 10 I=1,18                                                       ICDMOD26
```

```
     1          CRKSTR(6),STRESS(4),STRAIN(4),C(4,4),NODS(1),TEMPV1(1),  CDMOD 53

     2          TEMPV2(1),YZ(1),NOD5(1),WA(1),DUMWA(18)                  CDMOD 54

      DO 1 I=1,18                                                        CDMOD 66

   47 CALL DCRACK (C,SIG,ANGLE,MODEL,ITYP2D,NUMCRK,1,1,CRKSTR)           CDMOD270

      CALL DCRACK (C,STRESS,ANG,MODEL,ITYP2D,NUMCRK,1,2,CRKSTR)          CDMOD302

      CALL DCRACK (C,STRESS,ANGLE,MODEL,ITYP2D,NUMCRK,2,2,CRKSTR)        CDMOD350

      CALL DCRACK (C,STRESS,ANGLE,MODEL,ITYP2D,NUMCRK,1,2,CRKSTR)        CDMOD374

      CALL DCRACK (C,STRESS,ANGLE,MODEL,ITYP2D,NUMCRK,1,2,CRKSTR)        CDMOD422

      CALL DCRACK (C,STRESS,ANGPRI,MODEL,ITYP2D,NUMCRK,1,2,CRKSTR)       CDMOD427

      CALL DCRACK (C,STRESS,ANG,MODEL,ITYP2D,NUMCRK,2,1,CRKSTR)          CDMOD590

      DO 210 I=1,18                                                      CDMOD596


      DIMENSION STR(4),EPS(4),CRKSTR(6),SP1(1),SP31(1),SP32(1),SP33(1),  CRAKID15


      DIMENSION C(4,4),SIG(4),D(4,4),T(4,4),DSIG(4),CRKSTR(6)            DCRACK 9

C     RELEASE APPROPRIATE STRESSES                                       DCRAC204
C                                                                        DCRAC205
   98 NF=NUMCRK + 1                                                      DCRAC206
      GO TO (140,120,110,155,100,100,100), NF                            DCRAC207
  100 CALL DSOF (4,SIGP,FALSTR,EP,CRKSTR,E,VNU,SIGMAT,SIGMAC)            DCRAC208
      IF (NUMCRK - 5) 140,120,110                                        DCRAC209
  110 CALL DSOF (2,SIGP,FALSTR,EP,CRKSTR,E,VNU,SIGMAT,SIGMAC)            DCRAC210
  120 SIGP(3)=SIGP(3)                                                    DCRAC211
      CALL DSOF (1,SIGP,FALSTR,EP,CRKSTR,E,VNU,SIGMAT,SIGMAC)            DCRAC212
C                                                                        DCRAC213
C     ROTATE STRESSES TO GLOBAL AXES                                     DCRAC214
```

```
      SUBROUTINE DSOF (IJ,SIGP,FALSTR,EP,CRKSTR,E,VNU,SIGMAT,SIGMAC)
      IMPLICIT DOUBLE PRECISION ( A-H,O-Z )
      COMMON /SOFT/ ISCODE,WWCC,GGFF,DDAA,ELWW
      DIMENSION SIGP(4),EP(4),CRKSTR(6),CORN(11,3)
      IF (CRKSTR(IJ).GT.0.D0) GOTO 5
      SIGP(IJ)=FALSTR
      RETURN
    5 CONTINUE
C
      DATA (CORN(I,1),I=1,11)/0.,.05,.1,.15,.2,.25,.3,.4,.6,.8,1.0/
      DATA (CORN(I,2),I=1,11)/1.,.7082,.5108,.3817,.2986,.2446,
     1                       .2080,.1596,.0904,.0361,0.0/
      JJ=IJ
      IF (JJ.EQ.4) JJ=3
      KK=JJ+3
      EEPP=EP(IJ)
      IF (EP(IJ).GT.CRKSTR(KK)) CRKSTR(KK)=EP(IJ)
      IF (EP(IJ).LT.CRKSTR(KK)) EEPP=CRKSTR(KK)
      ISS=ISCODE-2
      IF (ISS) 10,20,30
C
   10 CONTINUE
      EETT=1/(1/E-(2*GGFF)/(SIGMAT**2*WWCC))
      SIGP(IJ)=FALSTR+EETT*(EEPP-CRKSTR(JJ))
      IF (EP(IJ).LT.CRKSTR(KK)) SIGP(IJ)=EP(IJ)/EEPP*SIGP(IJ)
      IF (SIGP(IJ).GT.FALSTR) SIGP(IJ)=FALSTR
      IF (SIGP(IJ).LT.0.D0) SIGP(IJ)=0.D0
      SIGP(3)=0.D0
      RETURN
C
   20 CONTINUE
      EO=GGFF/(WWCC*0.19704*SIGMAT)
      DO 21 I=1,11
      CORN(I,3)=CORN(I,1)+CORN(I,2)*CRKSTR(JJ)/EO
      IF (EEPP/EO.LT.CORN(I,3)) GO TO 22
   21 CONTINUE
   22 AA=(CORN(I-1,2)-CORN(I,2))/(CORN(I-1,3)-CORN(I,3))
      BB=CORN(I-1,2)-AA*CORN(I-1,3)
      SIGP(IJ)=FALSTR*(AA*EEPP/EO+BB)
      IF (EP(IJ).LT.CRKSTR(KK)) SIGP(IJ)=EP(IJ)/EEPP*SIGP(IJ)
      IF (SIGP(IJ).GT.FALSTR) SIGP(IJ)=FALSTR
      IF (SIGP(IJ).LT.0.D0) SIGP(IJ)=0.D0
      SIGP(3)=0.D0
      RETURN
C
   30 CONTINUE
      RETURN
C
      END
```

Appendix C

CRACK BAND MODEL, THREE-DIMENSIONAL

An additional card is needed (3-D solid elements, material 5, card d) with the same information as for the 2-D case.

<u>CHANGES IN THREDM.F77</u>

```
                                                                     Change at
                                                                     or after:
                                                                     ---------

    1     IDWAS / 0, 0, 0, 25,25, 0,14,21,21,47,47,38,8*0/,          THRED100

      COMMON /SOFT/ ISCODE,WWCC,ELWW,GGFF,DDAA                       THDFE 46

      IF (MODEL.EQ.5) READ(IIN,1009) ISCODE,WWCC,ELWW,GGFF,DDAA      THDFE102

 1009 FORMAT (I5,4F10.0)                                             THDF1190

      COMMON /SOFT/ ISCODE,WWCC,ELWW,GGFF,DDAA                       MATWRT14

      WRITE (6,2239)                                                 MATWR243

 2239 FORMAT(/38H (BB) CODE FOR TENSILE STRESS TRANSFER,I5,          MATWR596
    1        /38H         1=LINEAR SOFTENING           ,
    2        /38H         2=CORNELISSEN'S SOFTENING    ,
    3        /38H        SOFT BAND WIDTH (WWCC)        ,F10.5,
    4        /38H        SOFT ELEMENT WIDTH (ELWW)     ,F10.5,
    5        /38H        FRACTURE ENERGY (GGFF)        ,F10.8,
    6        /38H        MAXIMUM AGGREGATE SIZE (DDAA)  ,F10.5)
```

<u>CHANGES IN ELT3D4.F77</u>

```
      IDW=25*ITWO                                                    ELT3D444

      DIMENSION PROP(1),WA(25,1),XYZ(1),NOD9(1),NODS(1),TEMPV1(1)    ICMOD316

      DO 10 I=1,25                                                   ICMOD326

    1          CRKSTR(6),STRESS(6),STRAIN(6),C(6,6),RLMN(3,3),NODS(1), CMOD3D54
```

```
     1          TEMPV1(1),TEMPV2(1),XYZ(1),NOD9(1),WA(1),DUMWA(25)      CMOD3D55

      DO 1 I=1,25                                                      CMOD3D67

   47 CALL DCRAK3 (C,SIG,RLMN,MODEL,NUMCRK,1,1,CRKSTR)                 CMOD3261

      CALL DCRAK3 (C,STRESS,RLMN,MODEL,NUMCRK,1,2,CRKSTR)              CMOD3286

      CALL DCRAK3 (C,STRESS,RLMN,MODEL,NUMCRK,2,2,CRKSTR)              CMOD3340

      CALL DCRAK3 (C,STRESS,RLMN,MODEL,NUMCRK,1,2,CRKSTR)              CMOD3363

  159 CALL DCRAK3 (C,STRESS,RLMN,MODEL,NUMCRK,1,2,CRKSTR)              CMOD3414

      CALL DCRAK3 (C,STRESS,RLMN,MODEL,NUMCRK,1,2,CRKSTR)              CMOD3420

  130 CALL DCRAK3 (C,SIG,RLMN,MODEL,NUMCRK,2,1,CRKSTR)                 CMOD3561

      DO 210 I=1,25                                                    CMOD3567


      DIMENSION STR(4),EPS(4),CRKSTR(6),SP1(1),SP31(1),SP32(1),SP33(1), CRAKID15


      DIMENSION C(4,4),SIG(4),D(4,4),T(4,4),DSIG(4),CRKSTR(6)          DCRACK 9


C     RELEASE APPROPRIATE STRESSES                                     DCRAK165
C                                                                      DCRAK166
      NF=IK + 1                                                        DCRAK167
      GO TO (140,120,110,100,155), NF                                  DCRAK168
  100 CALL DSOF3 (3,SIGP,FALSTR,EP,CRKSTR,E,VNU,SIGMAT,SIGMAC)         DCRAK169
  110 SIGP(6)=SIGP(6)                                                  DCRAK170
      CALL DSOF3 (2,SIGP,FALSTR,EP,CRKSTR,E,VNU,SIGMAT,SIGMAC)         DCRAK171
  120 SIGP(5)=SIGP(5)                                                  DCRAK172
      SIGP(4)=SIGP(4)                                                  DCRAK173
      CALL DSOF3 (1,SIGP,FALSTR,EP,CRKSTR,E,VNU,SIGMAT,SIGMAC)         DCRAK174
C                                                                      DCRAK175
C     ROTATE STRESSES TO GLOBAL AXES                                   DCRAK176
```

```
      SUBROUTINE DSOF3 (IJ,SIGP,FALSTR,EP,CRKSTR,E,VNU,SIGMAT,SIGMAC)   DSOF3  2
      IMPLICIT DOUBLE PRECISION ( A-H,O-Z )
      COMMON /SOFT/ ISCODE,WWCC,GGFF,DDAA,ELWW
      DIMENSION SIGP(4),EP(4),CRKSTR(6),CORN(11,3)
      IF (CRKSTR(IJ).GT.0.D0) GOTO 5
      SIGP(IJ)=FALSTR
      RETURN
    5 CONTINUE
C
      DATA (CORN(I,1),I=1,11)/0.,.05,.1,.15,.2,.25,.3,.4,.6,.8,1.0/
      DATA (CORN(I,2),I=1,11)/1.,.7082,.5108,.3817,.2986,.2446,.2080,
     1                          .1596,.0904,.0361,0.0/
      JJ=IJ
      KK=JJ+3
      EEPP=EP(IJ)
      IF (EP(IJ).GT.CRKSTR(KK)) CRKSTR(KK)=EP(IJ)
      IF (EP(IJ).LT.CRKSTR(KK)) EEPP=CRKSTR(KK)
      ISS=ISCODE-2
      IF (ISS) 10,20,30
C
   10 CONTINUE
      EETT=1/(1/E-(2*GGFF)/(SIGMAT**2*WWCC))
      SIGP(IJ)=FALSTR+EETT*(EEPP-CRKSTR(JJ))
      IF (EP(IJ).LT.CRKSTR(KK)) SIGP(IJ)=EP(IJ)/EEPP*SIGP(IJ)
      IF (SIGP(IJ).GT.FALSTR) SIGP(IJ)=FALSTR
      IF (SIGP(IJ).LT.0.D0) SIGP(IJ)=0.D0
      IF (IJ-2) 12,11,11
   11 SIGP(6)=0.D0
   12 SIGP(5)=0.D0
      SIGP(4)=0.D0
      RETURN
C
   20 CONTINUE
      EO=GGFF/(WWCC*0.19704*SIGMAT)
      DO 23 I=1,11
      CORN(I,3)=CORN(I,1)+CORN(I,2)*CRKSTR(JJ)/EO
      IF (EEPP/EO.LT.CORN(I,3)) GO TO 24
   23 CONTINUE
   24 AA=(CORN(I-1,2)-CORN(I,2))/(CORN(I-1,3)-CORN(I,3))
      BB=CORN(I-1,2)-AA*CORN(I-1,3)
      SIGP(IJ)=FALSTR*(AA*EEPP/EO+BB)
      IF (SIGP(IJ).GT.FALSTR) SIGP(IJ)=FALSTR
      IF (SIGP(IJ).LT.0.D0) SIGP(IJ)=0.D0
      IF (IJ-2) 22,21,21
   21 SIGP(6)=0.D0
   22 SIGP(5)=0.D0
      SIGP(4)=0.D0
      RETURN
C
   30 CONTINUE
      RETURN
C
      END
```

DISTRIBUTION LIST

AF 6550 CES/DEEE, Patrick AFB, FL
AFESC HQ (library), Tyndall AFB, FL
ARMY 20th QM CO, 2nd QM Gp, Diving Sec, Taegu, Korea; CECOM R&D Tech Lib, Ft Monmouth, NJ
ARMY BELVOIR R&D CEN STRBE-AALO, Ft Belvoir, VA; STRBE-BLORE, Ft Belvoir, VA
ARMY CERL Library, Champaign, IL
ARMY CRREL Library, Hanover, NH
ARMY ENGR DIST Phila, Lib, Philadelphia, PA
ARMY MISSILE R&D CMD Ch, Docs, Sci Info Ctr, Arsenal, AL
BUREAU OF RECLAMATION D-1512 (GS DePuy), Denver, CO; Smoak, Denver, CO
CBC Library, Davisville, RI
CBU 411, OIC, Norfolk, VA
CNR Arlington, VA
COGARD R&DC Library, Groton, CT
COMDT COGARD Library, Washington, DC
DIA DB-6E1, Washington, DC; DB-6E2, Washington, DC; VP-TPO, Washington, DC
DIRSSP Tech Lib, Washington, DC
DNA STTI/TL, Washington, DC
DTIC Alexandria, VA
DTRCEN Code 4111, Bethesda, MD
GIDEP OIC, Corona, CA
LIBRARY OF CONGRESS Sci & Tech Div, Washington, DC
NBS Bldg Mat Div (Mathey), Gaithersburg, MD
NAVCOASTSYSCEN Tech Library, Panama City, FL
NAVEODTECHCEN Tech Library, Indian Head, MD
NAVFACENGCOM Code 03, Alexandria, VA; Code 04A, Alexandria, VA; Code 04A1D, Alexandria, VA; Code 04A3, Alexandria, VA; Code 04A4E, Alexandria, VA; Code 04B2 (J. Cecilio), Alexandria, VA; Code 0631, Alexandria, VA; Code 1002B, Alexandria, VA; Code 1651, Alexandria, VA
NAVFACENGCOM - CHES DIV, FPO-1PL, Washington, DC
NAVFACENGCOM - LANT DIV, Library, Norfolk, VA
NAVFACENGCOM - NORTH DIV, Code 04AL, Philadelphia, PA
NAVFACENGCOM - PAC DIV, Library, Pearl Harbor, HI
NAVFACENGCOM - SOUTH DIV, Library, Charleston, SC
NAVFACENGCOM - WEST DIV, Code 04A2.2 (Lib), San Bruno, CA
ARMY ENGR DIST Library, Seattle, WA
NAVCHAPGRU Code 60, Williamsburg, VA
NAVFACENGCOM Code 00, Alexandria, VA; Code 031 (Essoglou), Alexandria, VA; Code 04A1, Alexandria, VA; Code 07A (Herrmann), Alexandria, VA; Code 07M (Gross), Alexandria, VA; Code 09M124 (Lib), Alexandria, VA
NAVFACENGCOM - LANT DIV, Br Ofc, Dir, Naples, Italy
NAVOCEANSYSCEN DET, Tech Lib, Kailua, HI
NAVSHIPYD Code 202.4, Long Beach, CA; Library, Portsmouth, NH
NAVSWC Code E211 (Miller), Dahlgren, VA; Code W42 (GD Haga), Dahlgren, VA; PWO, Dahlgren, VA
PACMISRANFAC HI Area, PWO, Kekaha, HI
PMTC Code 1018, Point Mugu, CA
PWC ACE Office, Norfolk, VA; Code 101 (Library), Oakland, CA; Code 123-C, San Diego, CA; Code 420, Great Lakes, IL; Library (Code 134), Pearl Harbor, HI; Library, Guam, Mariana Islands; Library, Norfolk, VA; Library, Pensacola, FL; Library, Yokosuka, Japan; Tech Library, Subic Bay, RP
US DEPT OF INTERIOR Natl Park Svc, RMR/PC, Denver, CO
CALIFORNIA Nav & Ocean Dev (Armstrong), Sacramento, CA
CLARKSON COLL OF TECH CE Dept (Batson), Potsdam, NY
COLORADO SCHOOL OF MINES Dept of Engrg (Chung), Golden, CO
COLORADO STATE UNIVERSITY CE Dept (W Charlie), Fort Collins, MD
CORNELL UNIVERSITY Civil & Environ Engrg (Dr. Kulhawy), Ithaca, NY; Library, Ithaca, NY
DUKE UNIVERSITY CE Dept (Muga), Durham, NC
FLORIDA ATLANTIC UNIVERSITY Ocean Engrg Dept (Hart), Boca Raton, FL; Ocean Engrg Dept (McAllister), Boca Raton, FL; Ocean Engrg Dept (Su), Boca Raton, FL
FLORIDA INST OF TECH CE Dept (Kalajian), Melbourne, FL; CE Dept (Schwalbe), Melbourne, FL
JOHNS HOPKINS UNIV CE Dept (Jones), Baltimore, MD; Ches Bay Rsch Inst, Rsch Lib, Shady Side, MD
LAWRENCE LIVERMORE NATL LAB FJ Tokarz, Livermore, CA; Plant Engrg Lib (L-654), Livermore, CA
LEHIGH UNIVERSITY Linderman Library, Bethlehem, PA
MIT Engrg Lib, Cambridge, MA
NATL ACADEMY OF SCIENCES NRC, Naval Studies Bd, Washington, DC
OKLAHOMA STATE UNIV CE Scol (Lloyd), Stillwater, OK
PENNSYLVANIA STATE UNIVERSITY Applied Rsch Lab, State College, PA

PURDUE UNIVERSITY Engrg Lib, W. Lafayette, IN
STATE UNIVERSITY OF NEW YORK CE Dept, Buffalo, NY
TEXAS A&I UNIVERSITY Civil & Mech Engr Dept (Parate), Kingsville, TX
TEXAS A&M UNIVERSITY Ocean Engr Proj, College Station, TX
UNIV OF TENNESSEE CE Dept (Kane), Knoxville, TN
UNIVERSITY OF CALIFORNIA Engrg Lib., Berkeley, CA
UNIVERSITY OF DELAWARE CE Dept, Ocean Engrg (Dalrymple), Newark, DE; Engrg Col (Dexter), Lewes, DE
UNIVERSITY OF HAWAII Manoa, Library, Honolulu, HI
UNIVERSITY OF ILLINOIS Library, Urbana, IL; Metz Ref Rm, Urbana, IL
UNIVERSITY OF RHODE ISLAND CE Dept (Kovacs), Kingston, RI
UNIVERSITY OF TEXAS CE Dept (R Olson), Austin, TX; CE Dept (Thompson), Austin, TX
UNIVERSITY OF CALIFORNIA CE Dept (Fenves), Berkeley, CA
UNIVERSITY OF TEXAS Construction Industry Inst, Austin, TX
UNIVERSITY OF WASHINGTON CE Dept (N. Hawkins), Seattle, WA
WESTERN ARCHEOLOGICAL CEN Library, Tucson, AZ
AMERICAN SYS ENGRG CORP B. Williamson, Virginia Beach, VA
AMERICAN CONCRETE INSTITUTE Library, Detroit, MI
BATTELLE New Eng Marine Rsch Lab, Lib, Duxbury, MA
LINDA HALL LIBRARY Doc Dept, Kansas City, MO
NEW ZEALAND NZ Concrete Rsch Assoc, Library, Porirua
PERRY OCEAN ENGRG R. Pellen, Riviera Beach, FL
TRW INC Engr Library, Cleveland, OH
WISS, JANNEY, ELSTNER, & ASSOC DW Pfeifer, Northbrook, IL

INSTRUCTIONS

The Naval Civil Engineering Laboratory has revised its primary distribution lists. The bottom of the label on the reverse side has several numbers listed. These numbers correspond to numbers assigned to the list of Subject Categories. Numbers on the label corresponding to those on the list indicate the subject category and type of documents you are presently receiving. If you are satisfied, throw this card away (or file it for later reference).

If you want to change what you are presently receiving:

- Delete - mark off number on bottom of label.
- Add - circle number on list.
- Remove my name from all your lists - check box on list.
- Change my address - line out incorrect line and write in correction (**DO NOT REMOVE LABEL**).
- Number of copies should be entered after the title of the subject categories you select.

Fold on line below and drop in the mail.

Note: Numbers on label but not listed on questionnaire are for NCEL use only, please ignore them.

Fold on line and staple.

DEPARTMENT OF THE NAVY

Naval Civil Engineering Laboratory
Port Hueneme, CA 93043-5003

Official Business
Penalty for Private Use, $300

NO POSTAGE
NECESSARY
IF MAILED
IN THE
UNITED STATES

BUSINESS REPLY CARD

FIRST CLASS PERMIT NO. G-8

POSTAGE WILL BE PAID BY ADDRESSEE

Commanding Officer
Code L34
Naval Civil Engineering Laboratory
Port Hueneme, California 93043-5003

DISTRIBUTION QUESTIONNAIRE

The Naval Civil Engineering Laboratory is revising its Primary distribution lists.

SUBJECT CATEGORIES

1 SHORE FACILITIES
2 Construction methods and materials (including corrosion control, coatings)
3 Waterfront structures (maintenance/deterioration control)
4 Utilities (including power conditioning)
5 Explosives safety
6 Aviation Engineering Test Facilities
7 Fire prevention and control
8 Antenna technology
9 Structural analysis and design (including numerical and computer techniques)
10 Protective construction (including hardened shelters, shock and vibration studies)
11 Soil/rock mechanics
14 Airfields and pavements

15 ADVANCED BASE AND AMPHIBIOUS FACILITIES
16 Base facilities (including shelters, power generation, water supplies)
17 Expedient roads/airfields/bridges
18 Amphibious operations (including breakwaters, wave forces)
19 Over-the-Beach operations (including containerization, materiel transfer, lighterage and cranes)
20 POL storage, transfer and distribution

28 ENERGY/POWER GENERATION
29 Thermal conservation (thermal engineering of buildings, HVAC systems, energy loss measurement, power generation)
30 Controls and electrical conservation (electrical systems, energy monitoring and control systems)
31 Fuel flexibility (liquid fuels, coal utilization, energy from solid waste)
32 Alternate energy source (geothermal power, photovoltaic power systems, solar systems, wind systems, energy storage systems)
33 Site data and systems integration (energy resource data, energy consumption data, integrating energy systems)
34 ENVIRONMENTAL PROTECTION
35 Hazardous waste minimization
36 Restoration of installations (hazardous waste)
37 Waste water management and sanitary engineering
38 Oil pollution removal and recovery
39 Air pollution

44 OCEAN ENGINEERING
45 Seafloor soils and foundations
46 Seafloor construction systems and operations (including diver and manipulator tools)
47 Undersea structures and materials
48 Anchors and moorings
49 Undersea power systems, electromechanical cables, and connectors
50 Pressure vessel facilities
51 Physical environment (including site surveying)
52 Ocean-based concrete structures
54 Undersea cable dynamics

TYPES OF DOCUMENTS

85 Techdata Sheets 86 Technical Reports and Technical Notes
83 Table of Contents & Index to TDS
82 NCEL Guides & Abstracts
91 Physical Security

☐ None– remove my name